Cross Spectral Density Propagated Throught a Circular Aperture in the Fresnel Approximation

Por:

José Guadalupe Suárez Romero

Tesis sometida como requisito parcial para obtener el grado de **Doctor en Ciencias en la especialidad de Optica** en el Instituto Nacional de Astrofísica, Optica y Electrónica.

Supervisada por:

Dr. Eduardo Tepichín Rodríguez
INAOE

Sta. Ma. Tonantzintla, Pue.

Diciembre 1999

Agradecimientos

Agradezco al Dr. Eduardo Tepichín Rodríguez por su valioso trabajo realizado como director de esta tesis.

Agradezco al Dr. Klaus Mielenz por los importantes comentarios recibidos durante el desarrollo del presente trabajo.

Doy muchas gracias al Dr. Gabriel Martínez Niconoff por haber leído esta tesis y por sus interesantes sugerencias que ayudaron a la mejor comprensión de la teoría.

Quiero también agradecer al Dr. Mario Lehman por la lectura que hizo a este trabajo y por los varios comentarios que sirvieron de complemento para esta tesis.

Agradezco mucho al Dr. Wolfgang Schmid por haber leído el presente trabajo y por sus comentarios críticos y constructivos para este trabajo.

Quiero también agradecer al Dr. Jorge Ojeda Castañeda por sus importantes comentarios a este trabajo y por haber revisado el ingles de esta tesis.

Finalmente quiero agradecer con mucho cariño a mi familia y en particular a mi esposa Engracia Barraza Alvarado por toda la comprensión y apoyo que recibí de ellos durante el largo tiempo dedicado a este trabajo.

Index

Resumen

Introducción

La labor principal de un laboratorio nacional de metrología es la de establecer las unidades del sistema de medición de su país. Para el caso de México, el laboratorio en cuestión es el centro nacional de metrología (CENAM), y el sistema adoptado es el sistema internacional de unidades (SI).

En particular la radiometría se encarga de establecer las unidades de medición de variables ópticas. Las magnitudes radiométricas que nos interesan en este trabajo son la radiancia [$W/(c\,m^2\ sr)$] y la irradiancia [W/cm^2], las cuales serán implementadas en el CENAM.

Un patrón primario de radiancia es el radiador de cuerpo negro. Su radiancia es conocida y esta dada por la ley de Plank. Sin embargo un radiador de cuerpo negro es un instrumento costoso tanto en su adquisición como en su operación. Además, la estabilidad que éste alcanza en su emisión limita la incertidumbre que se puede alcanzar en las mediciones.

Un sistema alterno para materializar una escala de radiancia es mediante un banco radiométrico con dos aberturas como el mostrado en la Fig. R.1. El banco radiométrico consta de las siguientes componentes; una lámpara, un detector de respuesta conocida y de dos aperturas colocadas entre la fuente y el detector.

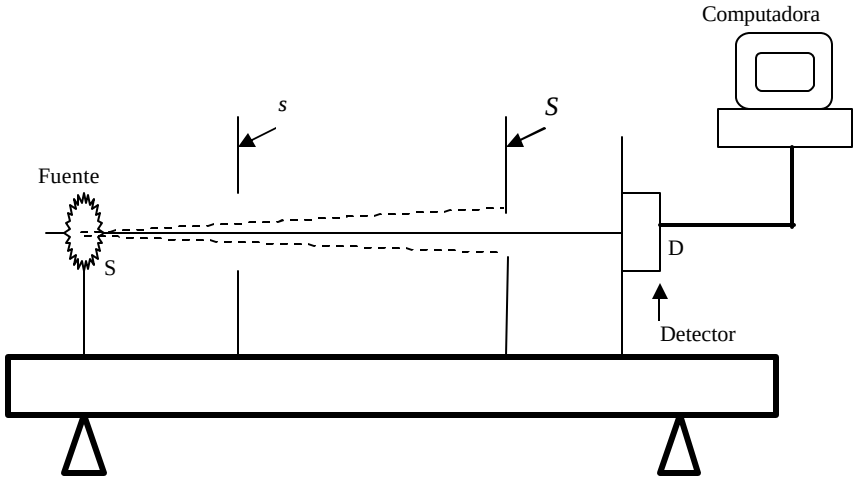

Fig. R.1. Banco Radiométrico.

La primera abertura limita la cantidad de luz que proviene de la lámpara y elimina casi por completo la luz extraviada que llega al detector. La segunda abertura define el cono de luz proveniente de la lámpara y que llegará al detector.

La proyección geométrica de la segunda abertura (*S*) sobre el plano del detector define los parámetros geométricos necesarios para el cálculo de la radiancia. Si la iluminación de la abertura es homogénea entonces el modelo de la radiancia se reduce a una expresión muy simple, dada en la siguiente expresión 1.

$$L = \frac{f}{AW}, \qquad \text{(R.1.)}$$

donde f es el flujo óptico que llega al detector considerando que toda la energía radiante se encuentra dentro de la zona iluminada y que en la sombra geométrica la energía es cero. A es el área de la fuente y W el ángulo sólido subtendido por la abertura S.

Sin embargo, este modelo geométrico de la radiancia sufre algunas desviaciones en el experimento, debido a la difracción en cada una de las aberturas. Dado que el modelo geométrico de la radiancia es el único modelo aceptado actualmente en los laboratorios primarios de metrología, debemos hacer correcciones a las mediciones de flujo que pasa a través de las aberturas. En una serie de publicaciones se discuten las correcciones que deben tomarse en cuenta debido a la redistribución de la irradiancia en el plano de detección por efectos de la difracción.

Para calcular las correcciones es necesario conocer la irradiancia en el detector. La irradiancia esta dada por el patrón de difracción de dos aberturas consecutivas e iluminadas por una fuente extendida monocromática incoherente.

Tal patrón de difracción no ha sido reportado por nadie (hasta donde sabemos), aunque existe una teoría general que da las bases para resolver este problema, conocida como la teoría de coherencia parcial. Por lo tanto, en este trabajo nos dedicamos a resolver el problema de la doble difracción por dos aberturas en aproximación de Fresnel, aplicando la teoría de coherencia parcial.

Teoría básica

En al teoría de coherencia espacial se generaliza el concepto de la irradiancia, la magnitud generalizada resultante se llama la intensidad mutua. A la intensidad mutua se le denota por $G(\boldsymbol{X}_1, \boldsymbol{X}_2, t)$,

donde $\boldsymbol{X}_1$, y $\boldsymbol{X}_2$ son vectores cuyas coordenadas describen los puntos del campo óptico que se están comparando, y t es la diferencia temporal entre los puntos $\boldsymbol{X}_1$, y $\boldsymbol{X}_2$.

Cuando evaluamos a la intensidad mutua en el mismo punto, $\boldsymbol{X}_1=\boldsymbol{X}_2$, regresamos al concepto de la irradiancia; $E(\boldsymbol{X}_1)= G(\boldsymbol{X}_1, \boldsymbol{X}_1, t)$. Otra magnitud importante en la teoría de coherencia espacial es la densidad espectral mutua, denotada por $W(X_1, X_2, w)$. Los vectores $\boldsymbol{X}_1$, y $\boldsymbol{X}_2$ son los mismos que para el caso de la intensidad mutua, y w es la frecuencia angular de la radiación óptica. La densidad espectral mutua es la transformada de Fourier de la intensidad mutua. Y las variables w y t son las variables conjugadas de la transformada de Fourier. De tal manera que las dos magnitudes están relacionadas por

$$W(\boldsymbol{X}_1, \boldsymbol{X}_2, w) = \Im\{G(\boldsymbol{X}_1, \boldsymbol{X}_2, t)\}. \tag{R1}$$

La propagación de la densidad espectral mutua esta dada por la siguiente ecuación integral cuatro dimensional,

$$W'(P_1, P_2, n) = \frac{1}{l^2}\int_{S_2}\int_{S_1} W(S_1, S_2, n)\cos(q_1)\cos(q_2)\frac{e^{ik(r_1-r_2)}}{r_1 r_2} dS_1 dS_2$$

donde W' es la densidad espectral mutua del campo propagado y W es la densidad espectral mutua del campo inicial, finalmente k es el número de onda. Para el caso que queremos resolver necesitamos dos propagaciones, por lo que aplicando dos veces la Ec. (R.2) tendremos

$$W''(U_1,U_2,n)=\frac{1}{l^4}\int_{Q_2}\int_{Q_1}\int_{P_2}\int_{P_1}W(P_1,P_2,n)\cos(q_1)\cos(q_2)\cos(q_1')\cos(q_2')\frac{e^{ik(P_1Q_1-P_2Q_2)}}{P_1Q_1\cdot P_2Q_2}\frac{e^{ik(Q_1U_1-Q_2U_2)}}{Q_1U_1\cdot Q_2U_2}dP_1dP_2dQ_1dQ_2 \tag{R.3}$$

donde *W*" es la densidad espectral mutua resultante de la segunda propagación. La Ec. (R.3) se encuentra reportada en la literatura y es nuestro punto de partida para resolver el problema planteado en la introducción.

Planteamiento del problema

La radiancia de una fuente plana extendida se define como la cantidad de flujo radiante que emite la fuente por unidad de área proyectada y por unidad de ángulo sólido, es decir,

$$L=\frac{df}{dA_{\perp}dW} \tag{R.4}$$

donde df es el diferencial de flujo radiante emitido por el diferencial de área proyectada $dA_{\perp}$ de la fuente en la dirección del diferencial de ángulo sólido dW.

En la Fig. R.1 la fuente S representa una fuente extendida lambertiana con una radiancia L que queremos medir. En el caso de fuentes lambertianas la emisión de radiación óptica es homogénea en toda la superficie de emisión de la fuente, por lo que el elemento de área puede ser toda la fuente. El ángulo sólido queda definido por la segunda abertura S, y el flujo radiante emitido en el ángulo sólido llega al detector D y es medido.

En una primera aproximación, con los datos anteriores podemos calcular la radiancia de la fuente dada por la Ec. (R.4). Sin embargo para mediciones de muy alta exactitud, éste modelo no es suficiente. Los efectos de la difracción tanto por la primera abertura s como por la segunda abertura S, pueden causar una concentración o una dispersión de la energía que pasa por la segunda abertura. Causando que la energía que llega al detector sea hasta un 0,5% diferente de la esperada si no hubiera ninguna pantalla con abertura.

El efecto de las aberturas se puede corregir conociendo el patrón de difracción en el detector. En este caso en particular necesitamos conocer el patrón de difracción (de Fresnel) de dos aberturas circulares sucesivas. Hasta donde sabemos, nadie a reportado tal patrón de difracción. Por lo que el objetivo de este trabajo es calcular dicho patrón de difracción.

El punto de partida es una ecuación integral ocho dimensional publicada por K. D. Mielenz, ya mencionada en la teoría básica, Ec. (R.4).

En la Fig. R.2, se muestra un esquema del banco radiométrico con la notación usada en el presente trabajo.

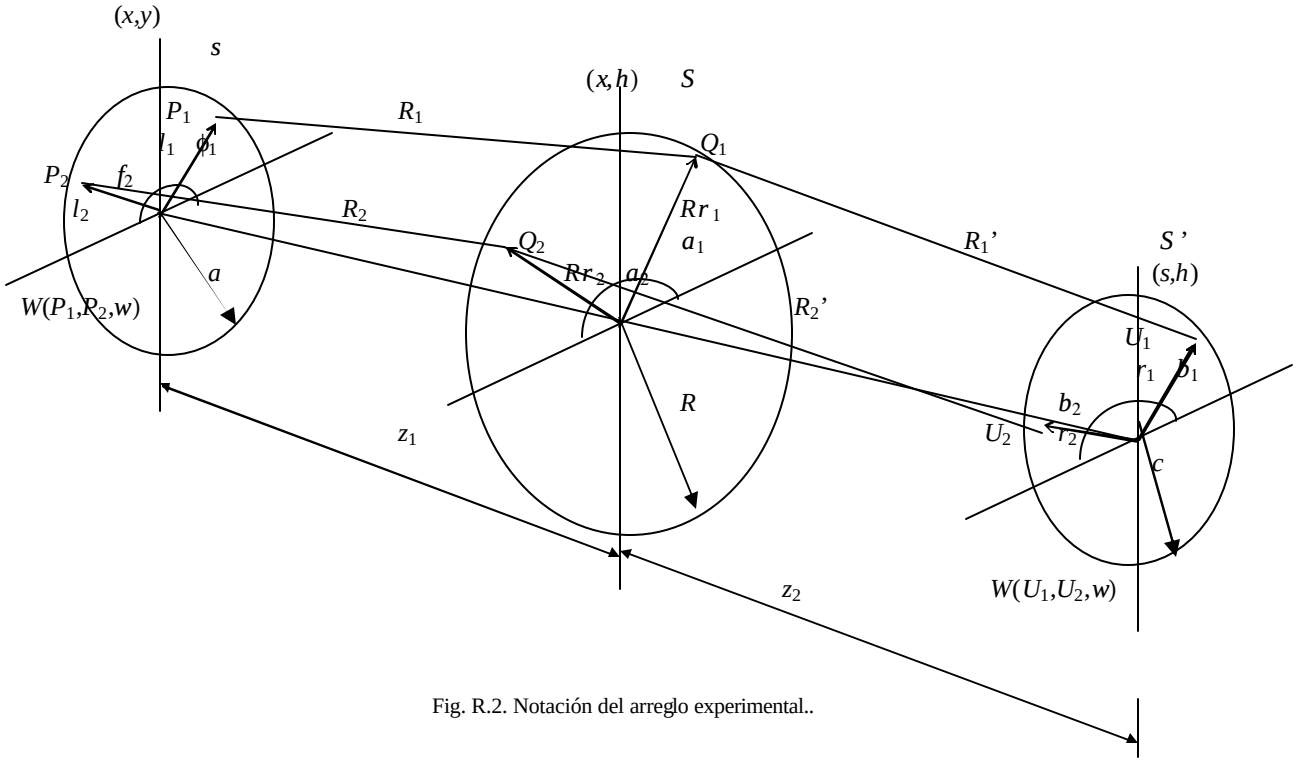

Fig. R.2. Notación del arreglo experimental..

Reescribiendo la Ec. (R.4) usando la notación de la Fig. R.2 tendremos

$$W(U_1,U_2,w)=\frac{1}{l^4}\int_{Q_2}\int_{Q_1}\int_{P_2}\int_{P_1}\frac{\cos(\boldsymbol{n},\boldsymbol{Q_1U_1})\cos(\boldsymbol{n},\boldsymbol{Q_2U_2})}{R_1'R_2'}\frac{\cos(\boldsymbol{n},\boldsymbol{P_1Q_1})\cos(\boldsymbol{n},\boldsymbol{P_2Q_2})}{R_1R_2}$$

$$W(P_1,P_2,w)e^{ik[R_1-R_2+R_1'-R_2']}dP_1dP_2dQ_1dQ_2 \quad .$$

(R.5)

La solución de esta ecuación es lo que ocupa al resto del presente trabajo. En la siguiente sección se muestra la forma en que se resolvió la Ec. (R.5).

Desarrollo

En el presente trabajo se muestra como la Ec. (R.5) puede ser resuelta mediante un cambio de variables en coordenadas polares fuera del origen.

Como primer paso se reduce la integral al caso de la aproximación de Fresnel, luego se hace un cambio de coordenadas polares. Posteriormente se hace un segundo cambio de variables para usar coordenadas polares normalizadas, mediante las siguientes definiciones

$$u = k \frac{z_1 + z_2}{z_1 z_2} R^2, \tag{R.6.1}$$

$$v_j = k \frac{R}{z_2} r_j, \quad j = 1, 2, \tag{R.6.2}$$

$$l'_j = \frac{kRl_j}{z_1}, \qquad j = 1, 2. \tag{R.6.3}$$

Usando las Ecs. (R.6) se puede reducir la integral (R.5) a la siguiente expresión

$$W(U_1,U_2,w)=\frac{R^4}{l^4 z_1^2 z_2^2}\, e^{i\frac{z_2}{2R^2k}\left[v_1^2-v_2^2\right]} \int_{Q_2}\int_{Q_1}\int_{P_2}\int_{P_1} W(P_1,P_2,w)\, e^{i\frac{u}{2}\left(r_1^2-r_2^2\right)}\, e^{i\frac{z_1}{2R^2k}\left(l_1'^2-l_2'^2\right)}$$

$$e^{i\left[\left(l_2'\cos f_2+v_2\cos b_2\right)r_2\cos a_2+\left(l_2'\sin f_2+v_2\sin b_2\right)r_2\sin a_2\right]}$$

$$e^{-i\left[\left(l_1'\cos f_2+v_1\cos b_1\right)r_1\cos a_1+\left(l_1'\sin f_2+v_1\sin b_1\right)r_1\sin a_1\right]}$$

$$\left(\frac{z_1}{kR}\right)^4 l_1' df_1 l_2' df_2 dl_1' dl_2' r_1 r_2 da_1 da_2 dr_1 dr_2 \ . \qquad \text{(R.7)}$$

Para continuar proponemos el siguiente cambio de variables, las cuales forman un sistema de coordenadas polares fuera del origen:

$$\begin{aligned} L_1\cos\Psi_1 &= l_1'\cos f_1 + v_1\cos b_1, \\ L_1\sin\Psi_1 &= l_1'\sin f_1 + v_1\sin b_1, \\ L_2\cos\Psi_2 &= l_2'\cos f_2 + v_2\cos b_2, \\ L_2\sin\Psi_2 &= l_2'\sin f_2 + v_2\sin b_2. \end{aligned} \qquad \text{(R.8)}$$

con sus correspondientes jacobianos

$$J_1 = \frac{L_1}{\left[L_1^2 + v_1^2 - 2L_1 v_1 \cos\left(Y_1 - b_1\right)\right]^{1/2}},$$
$$J_2 = \frac{L_2}{\left[L_2^2 + v_2^2 - 2L_2 v_2 \cos\left(Y_2 - b_2\right)\right]^{1/2}}. \tag{R.9}$$

Sustituyendo este cambio de variables se puede demostrar que la Ec. (R.7) se reduce a la siguiente expresión

$$W\left(U_1, U_2, w\right) = \iint W\left(P_1, P_2, w\right) K\left(U_1, P_1, w\right) K^*\left(U_2, P_2, w\right) dP_1 dP_2 \tag{R.10}$$

donde

$$K\left(\mathrm{l}', f; \mathrm{v}, b\right) = -\frac{1}{i l^2 z_1 z_2}\left(\frac{\mathrm{z}_1}{\mathrm{k}}\right)^2 \mathrm{e}^{\mathrm{i}\frac{z_1+z_2}{2R^2\mathrm{k}}\mathrm{v}^2}\ \mathrm{e}^{\mathrm{i}\frac{z_1}{R^2\mathrm{k}}\left[\frac{\mathrm{L}^2}{2} - \mathrm{L}\mathrm{v}\cos\left(Y - b\right)\right]}\left[C\left(\mathrm{u}, \mathrm{L}\right) - \mathrm{i}S\left(\mathrm{u}, \mathrm{L}\right)\right], \tag{R.11}$$

resultando ser la función de transferencia del sistema óptica. La Ec. (R.10) es la solución buscada. En la siguiente sección mostramos algunos ejemplos numéricos de la Ec. (R.10).

Ejemplos Numéricos

Se realizaron varios cálculos numéricos donde se muestran los efectos de difracción de las dos aberturas. En el primer ejemplo se calcula la distribución de irradiancia en el detector debido a una fuente puntual y una abertura. En el segundo ejemplo se calcula el caso de una fuente incoherente expandida. Y para el tercer caso se le agrega al segundo ejemplo una segunda abertura.

Los valores numéricos de los parámetros son los siguientes, se considera una fuente circular incoherente de radio a_0=0,3mm, una abertura s de radio a=4mm, y una abertura S de radio R=1,06mm. La distancia entre la fuente y la abertura s es z_0=1m, la distancia entre las aberturas s y S es z_1=1m, y finalmente la distancia entre la abertura S y el plano del detector es z_2=0,5m. La presente configuración corresponde a un valor de u en la Eq.(R.6.1) igual a u=28,9306. En el cálculo se usaron las expresiones dadas en la Ec. (4.24) ó (R.10). En el tercer caso la densidad espectral mutual en la abertura s esta dada por

$$W(P_1, P_2, w) = \frac{E_S}{z_0^2} \frac{2J_1(d)}{d} \exp[ij], \tag{R.12}$$

donde

$$d = \frac{z_1 a_0}{z_0 R} \sqrt{L_1^2 + L_2^2 - 2L_1 L_2 \cos(\Psi_1 - \Psi_2)}, \tag{R.13}$$

y

$$j = \frac{z_1^2}{2z_0 kR^2}\left[L_1^2 - L_2^2 - 2L_1 v\cos(\Psi_1) + 2L_2 v\cos(\Psi_2)\right], \qquad \text{(R.14)}$$

Y se ha aproximado el término exponencial a uno. Se muestra en la Fig. 4.8 los perfiles de irradiancia que se obtuvieron numéricamente; en la Fig. 4.8*A* se presenta el perfil de irradiancia en el detector para el primer caso, en la Fig. 4.8*B* se presenta el perfil correspondiente para el segundo caso, y finalmente en la Fig. 4.8*C* se presenta el tercer caso.

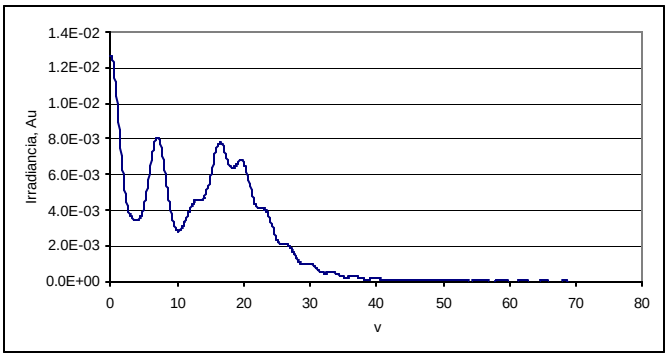

Fig. 4.8*A*. Distribución de irradiancia debido a una fuente puntual, u=28,9360.

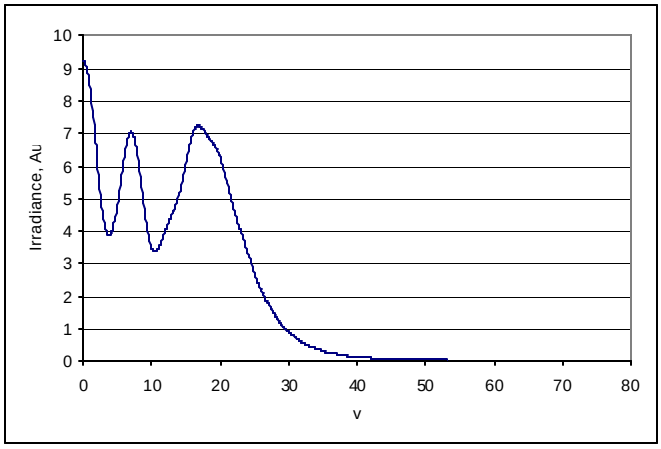

Fig. 4.8*B*. Distribución de irradiancia debido a una fuente incoherente extendida, u=28,9360.

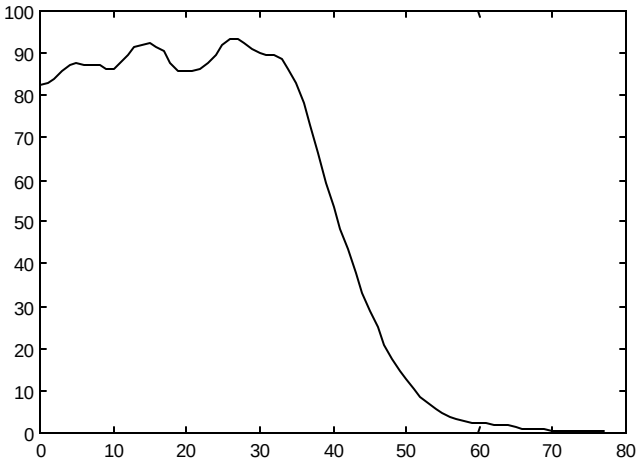

Fig. 4.8*C*. Distribución de irradiancia debido a la misma fuente incoherente extendiad y dos aberturas, u=28,9360.

Se observa que la diferencia en considerar una fuente puntual y una fuente extendida es un efecto de suavizado, figures 4.8*A* y 4.8*B*. Mientras que el uso de una segunda abertura intermedia (abertura *s*) produce efectos de difracción significativos.

Resultados Experimentales

Se realizo un experimento utilizando un patrón de radiancia. La fuente se ajustó a un diámetro de 0,5mm. Un filtro de banda angosta se usó para obtener luz cuasimonocromática. La abertura S, se colocó a una distancia z_1=1m, la cual tiene un diámetro de 2,12mm. El detector se colocó a una distancia z_2 = 0,56m (see Fig. 4.1). Esta configuración óptica corresponde a un valor de u en la Ec. (4.16.1) de 35,49.

Se muestra en la Fig. 5.2a la imagen de la irradiancia en el plano del detector. En la Fig. 5.2b se muestra el perfil normalizado de la irradiancia. El perfil se obtuvo de un varrido de perfiles de la fotografía del patron de irradiancia. El ruido que muestra el perfil es debido al proceso de escaneado

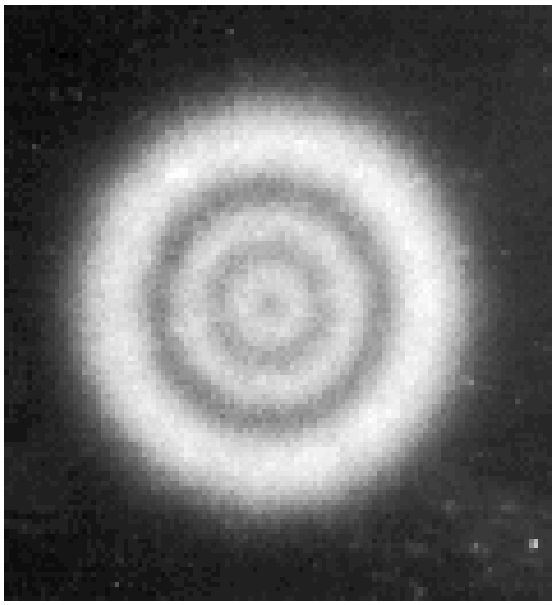

Fig. 5.2a. Resultado experimental para una fuente expandida de diámetro 0.5 mm con z_1=1m, z_2=0.56m, un diámetro de abertura de 2.12mm y una longitud de onda de 550nm.

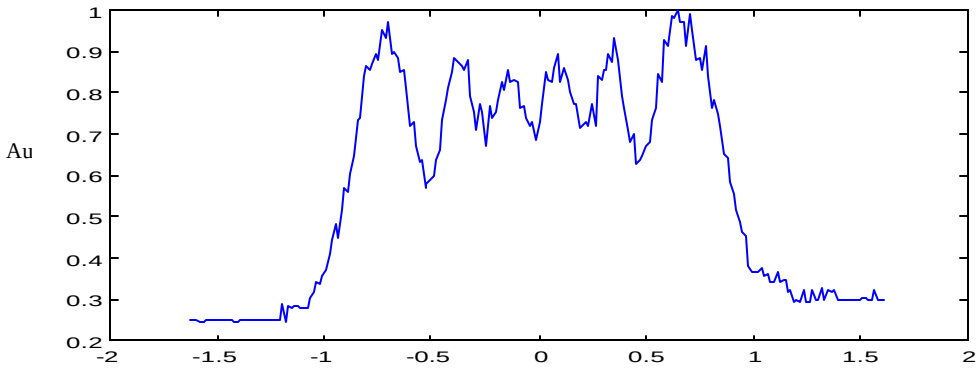

Fig. 5.2b. Perfil normalizado de la distribución de irradiancia experimental que se muestra en la Fig. 5.2a.

Se realizo en seguida el cálculo numérico de la irradiancia para esta configuración experimental usando la Ec (5.11). Se muestra en la Fig. 5.2c el perfil de irradiancia correspondiente. Notamos que a pesa del ruido ambos perfiles son practicamente los mismos.

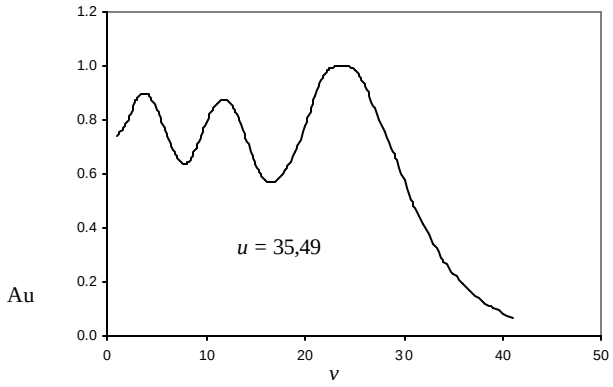

Fig. 5.2c. Evaluación numérica de la Ec. (5.11) usando los parámetros experimentales de la Fig. 5.2a.

Lo anterior muestra que nuestra ecuación simplificada (5.11) reproduce bastante bien los resultados experimentales. Esto es entonces una demostración de la consistencia de nuestros resultados analíticos.

Chapter 1.

1. Introduction.

The main task of a National Laboratory of Metrology is to establish, to preserve and to offer benchmarks for measurement, in industry and commerce. For radiometric measurements one also needs to establish a benchmark. The goal for establishing a radiometric standard is to understand the use of limiting apertures within an optical system. The use of those apertures is necessary to eliminate the stray light and to specify a measurement surface on a detector. For example, the radiance of a lamp can be measured with the help of a detector. We need to know the response of the detector as well as geometrical parameters: as the detection surface, the solid angle, the radiating surface of the lamp, distances, etc. All these parameters can be established with the help of apertures.

According to geometrical optics, an aperture selects a set of rays (coming from the source) into an illuminated zone and a shadow zone. Hence the illuminated zone is the geometrical projection of the aperture, see Fig. 1.1. If we assume an isotropic angular distribution (of the rays coming from the source), then the bright zone is uniformly illuminated. One can observe experimentally that along the projection of the edges, there is a penumbra. Here the illumination decays to zero. The extension of the penumbra is proportional to the size of the source.

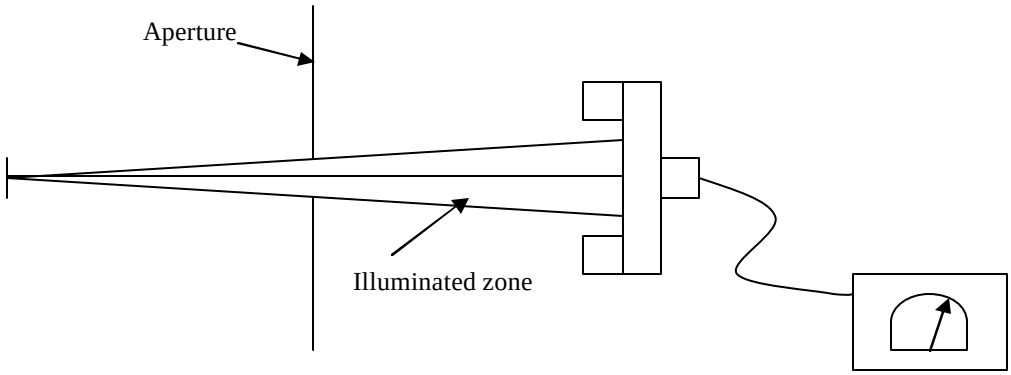

Fig. 1.1 Schematic diagram of the geometrical model.

However, this basic model (based on geometrical projections) is only useful until a limited level of accuracy. For high precision radiometry [1] one must take into account departures from the geometrical model. Consequently diffraction effects must be considered, see Fig. 1.2.

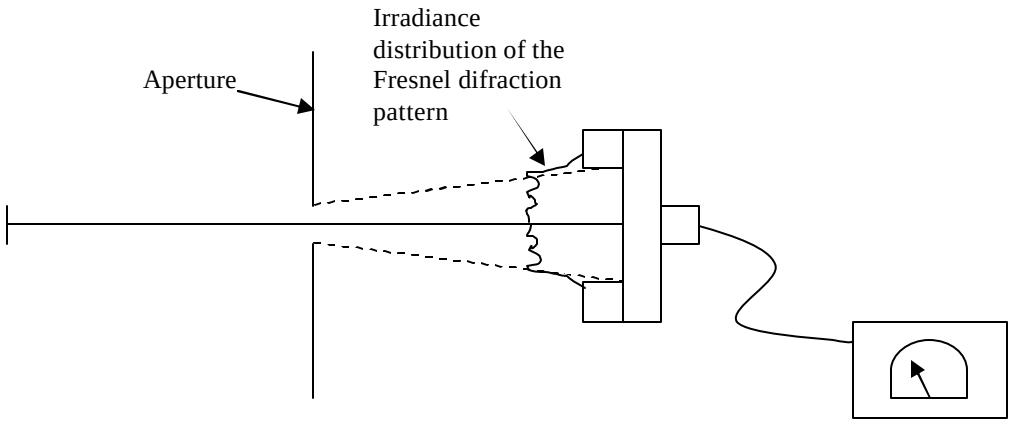

Fig. 1.2 Schematic diagram of the wave model.

Irradiance measurement, on the detector's plane, may be smaller than or bigger than those predicted by using the geometrical model.

[1] For example, in the establishment of national standards of radiance with lamps, or in the realization of the photometric unit the candela.

For example, on the one hand, Sanders et. al [1] and Blevin [2] reported that the flux density in the bright zone was smaller than the expected, by using purely geometrical considerations. On the other hand, Boivin [3] reported an excess of flux density.

Another interesting feature is the following. In the shadow zone the flux density is not strictly zero. And sometimes it is necessary to make an estimation of the proportion of light that goes out the detector. The departure from the geometrical model is a consequence of the diffraction effects of the edges of the aperture. The diffracted light is redistributed into both the bright zone, and the shadow zone. It is clear that errors in the measurements are significant if the diffraction effects are not considered.

For example, Sanders et al. employed Fraunhofer diffraction theory, for evaluating this effect. They found that the illumination at the center of the image was 0,25% smaller than that predicted by the geometrical optics. Two years later, this prediction was experimentally confirmed by Ooba [4].

In the case of Blevin, he reported that when measuring the Stefan-Boltsman's constant, there was a difference up to 0,5% between the measured value and the value predicted when using geometrical optics. Blevin, in his publication, makes a clear explanation of the problem. He stated that in case for very high accurate measurements it is necessary to apply a correction factor, to the radiance measurements due to the use of a limiting aperture. He proposed some approximations to evaluate these errors, from the viewpoint of radiometry.

Therefore, in radiometry the so-called "diffraction errors" are usually associated to any departure of the irradiance distribution (on the plane of the detector) from that obtained by using the geometrical model.

In the calculus of the correction factor, one needs to evaluate Fresnel diffraction of the aperture when it is illuminated by a point source. In this manner one obtains the Lommel's functions.

Now if one assumes that the extended source is composed by a collection of point sources, mutually incoherent to each other, then the irradiance distribution due to an extended source is obtained adding the irradiance distributions of all point sources.

An important limitation to the above approach is the following. The Lommel's functions are infinite series, that one needs to truncate. The accuracy of the truncation depends heavily of the geometry of the extended source; as well as on the form and position of the aperture.

Several researches have reported different approximations, which are valid for special geometrical arrangements. These approximations have been compiled to offer guidelines, when making radiometric measurements; see for instance references [5] to [10].

The above dilemma becomes more delicate if requires two or more apertures [3-10].

The calculus for a system with two apertures results in a form so complicate, that only some estimations are reported based on the model of one aperture and particular conditions are recommended where the diffraction errors due to a second aperture are minimized. For example, Boivin [3] in his system uses two apertures of radii 2,5 cm and 0,3 cm respectively. His experimental setup uses a tungsten lamp as the illuminating source. The radius of the first aperture is 2,5 cm. This aperture is located at 50cm after the

source, and 50 cm away the second aperture is placed finally, 20cm after the second aperture, the detector is located. The wave model predicts that the first aperture produces an excess of irradiance in the second aperture of approximately $(1 \pm 1{,}5) \times 10^{-5}$ per cent, of an oscillatory nature [3]. Furthermore, if one ignores the first aperture and evaluates the influence of only the second aperture, then the wave model predicts an error of $4{,}4 \times 10^{-4}$ per cent smaller that the irradiance expected in the detector. The difference between the two effects is a factor of 20. And consequently Boivin claims that the effect of the first aperture over the second one can be negligible.

In reference [3] evaluations are reported on the amount of energy that passes through the second aperture. Working hypothesis as the one proposed by Boivin are commonly used in radiometric considerations [3, 10]. To our knowledge, it does not exist numerical evaluations that take into account the presence of the whole set of apertures in an optical setup.

The main limitation to an approach that considers the whole set of apertures is that it does not exist a practical formulation for performing this type of evaluations.

Therefore, the aim of this work is to calculate the irradiance distribution in the plane of a detector taken into account two successive apertures. This formulation allows to calculate the corresponding correction factors. The main idea in our proposal is to consider the first aperture as a partially coherent source. Hence, we can apply the Theory of Partial Coherence to calculate the Cross Spectral Density in the plane of the detector. As a particular case, the irradiance distribution in the plane of the detector can be calculated with this formalism, which represent our main objective.

In order to achieve our goal, we have organized this work in the following manner. In chapter 2 and 3 we are going to review the fundaments of partial coherence theory. More than a formal discussion, chapters 2 and 3 are meant to set a common notation for this thesis.

In chapter 4 we establish the radiometric problem in terms of partial coherence theory. And then we obtain the general solution. We also discuss the general form of the transmission function of the two aperture system. In chapter 5 we analyze the interesting and important case of an incoherent source. We show also experimental results that confirm our calculations. Finally, in chapter 6, we summarize our work with some conclusions.

CHAPTER 2

Partial Coherence Theory.

2.1 Partial Coherence Theory.

In this section we will review some aspects of the theory of Partial Coherence as well as important definitions useful for this work. We begin by pointing out the following. In principle, Maxwell's electromagnetic theory is a rigorous mathematical treatment for explaining the macroscopic phenomena of electromagnetic fields, and in particular of optical fields. However, if we have a system formed by a big number of electromagnetic components, then the rigorous solution is practically impossible to be handle. A better approach is to treat such systems with a statistical theory.

One example where we see the statistical character of radiometric quantities is the optical irradiance. This concept has only an average meaning, since it is the time average of the electric (or magnetic) vector. In partial coherence, this quantity finds a natural generalization.

Partial Coherence theory deals with the statistical aspects of electromagnetic phenomena. This theory can help us to obtain a better approximation of the average process observed in many optical systems. Two formulations of the partial coherence theory have been reported; one due to Wolf in 1955 [11] and other given by of Blanc-Lapierre and Dumontet also in 1955 [12]. The essential difference between these two formulations is that Wolf treats the subject in terms of complex functions as introduced by Gabor [13], whereas Blanc-Lapierre and Dumontet deal mainly with real functions. We use here the generalization given by Wolf. This formulation begins with the concept of analytic signals, which we define in the next section.

2.2. **Analytic Signal.**

As mentioned above, there are two Formulations of the Theory of Partial Coherence. Both formulations are rigorous and general. The difference between them is that the one given by Wolf treats the subject with carefully defined complex functions as we will see in this chapter, whereas in the second work, Blanc-Lapierre and Dumontet treat with real functions.

In Wolf's formulation the real signal of an electromagnetic field is associated with an analytic signal. The analytic signal was introduced by Gabor [13] to treat problems arising in communication theory. This is a generalization of the strict monochromatic case, where we associate to a real function a monochromatic complex function. In the case of analytic signals, they are an association to polychromatic fields.

Since the importance of analytic signals in our discussion, we summary, in what follows, the main features of the analytical signals. For a thorough discussion, to refer to [14] and [15].

Let $V^r(t)$ be a real function of the real variable t such that it possesses a Fourier transform, which we denote by $\mathbf{V}^r(w)$. Hence the real function can be written as

$$V^r(t) = \frac{1}{2p}\int_{-\infty}^{\infty}\mathbf{V}^r(w)e^{-itw}dw\ ; \tag{2.1}$$

where $\mathbf{V}^r(w) = [\mathbf{V}^r(-w)]^*$; it is a hermitian function.

Consequently, from the inversion theorem of the Fourier transform, we have that

$$\mathbf{V}^r(w) = \int_{-\infty}^{\infty}V^r(t)e^{iwt}dt\ . \tag{2.2}$$

Now, let $a(w)$ and $f(w)$ be two real functions such that the Fourier transform $\mathbf{V}^r(w)$ can be written in the form

$$\mathbf{V}^r(w) = a(w)e^{if(w)} = \left[\mathbf{V}^r(-w)\right]^* = a(-w)e^{-if(-w)}; \tag{2.3a}$$

hence

$$a(w) = a(-w), \quad f(w) = -f(-w). \tag{2.3b}$$

If we substitute Eq. (2.3) in Eq. (2.1) we obtain that

$$V^r(t) = \frac{1}{p}\int_0^\infty a(w)\cos[-wt + f(w)]dw\,. \tag{2.4}$$

Thus, any real function that has a Fourier transform can be represented as a Fourier cosine integral. The physical implication of this result is simply that all the information about the real function is contained in the positive (or negative) frequencies only.

We now define a new real function $V^i(t)$ by changing the cosine by sine in the integral of Eq. (2.4), that is

$$V^i(t) = \frac{1}{p}\int_0^\infty a(w)\sin[-wt + f(w)]dw\,. \tag{2.5}$$

The difference between Eq. (2.4) and Eq. (2.5) is a phase constant $p/2$. In terms of this function, the analytic signal $V(t)$ associated with the real function $V^r(t)$ may be defined as

$$V(t) = V^r(t) + iV^i(t). \tag{2.6}$$

Or expressed in terms of frequency

$$V(t) = \frac{1}{p}\int_0^\infty a(w)e^{-i[wt - f(w)]}dw = \frac{1}{2p}\int_0^\infty \mathbf{V}(w)e^{-iwt}dw\ , \tag{2.7}$$

where $\mathbf{V}(w) = 2\mathbf{V}^r(w)$, see Eq. (2.2). From Eq. (2.7) it is clear that the analytic signal representation is simply a generalization to polychromatic fields of the technique of replacing a cosine by an exponential for simply periodic functions (monochromatic wave). In other words, $\mathbf{V}(w)$ represents the spectrum of a polychromatic optical field, w is the angular frequency, $w = 2\ p/\ \lambda$, $V(t)$ is the irradiance of the polychromatic optical field, t is the time. Note also that the analytic signal contains only positive frequencies, which is an important property for a representation of a real disturbance. From Eq. (2.7), the inversion theorem for analytic signals gives

$$\begin{aligned} \mathbf{V}(w) &= \int_{-\infty}^{\infty} V(t)e^{iwt}dt \qquad w \geq 0, \\ &= 0 \qquad\qquad\qquad\quad w < 0. \end{aligned} \tag{2.8}$$

Other equivalent way to define analytic signals is with the Hilbert transforms theory as follow. Let us again $V^r(t)$ be any real function such that its Hilbert transform exist, which we will denote by

$$H\left[V^r(t)\right]=\frac{1}{p}P\int_{-\infty}^{\infty}\frac{V^r(t')}{t'-t}dt', \tag{2.9}$$

where the symbol P denotes Cauchy's principal value. In terms of Hilbert transforms, an analytical signal $V(t)$ associated with $V^r(t)$ is defined as

$$V(t)=V^r(t)+iH\left[V^r(t)\right]. \tag{2.10}$$

The equivalence between both definitions is not difficult to demonstrate [16]. The main argument is that the function $V^i(t)$ as defined in Eq. (2.5) is related to $V^r(t)$ by means of a Hilbert transform, that is

$$V^i(t)=\frac{1}{p}P\int_{-\infty}^{\infty}\frac{V^r(t')}{t'-t}dt'. \tag{2.11}$$

The definition of analytical signals with Hilbert transforms gives a useful notation to define the Cross Correlation of analytical signals. Such definition is the subject of the next section.

2.3. **Cross-Correlation of an analytical signal.**

The cross-correlation of two complex functions f_1 and f_2 is typically defined as

$$y_{12}(t) = \lim_{T\to\infty} \frac{1}{2T} \int_{-T}^{T} f_1^*(t)\, f_2(t+t)dt\,, \tag{2.12}$$

where t is only an integration variable and t is a translation of the coordinate t.

In the case of analytical signals we need to proceed as follows: Let $V^r(\mathbf{r},t)$ represents some polychromatic optical field. The function $V^r(\mathbf{r},t)$ can be defined in all the temporal space. To assure that the Hilbert transform of the function $V^r(\mathbf{r},t)$ exist, and that the Hilbert transform is square integrable (at least in a finite interval), we define the following real function (see reference [14]);

$$V_{2T}^{r}(\mathbf{r},t) = V^{r}(\mathbf{r},t)\,rect\left[\frac{t}{2T}\right] \quad . \tag{2.13a}$$

Since $V^{r}(\mathbf{r},t)$ is finite in all the space, then the function of Eq. (2.13a) is square integrable. Lets $V^{i}_{(2T)}(\mathbf{r},t)$ be the Hilbert transform of $V^{r}{}_{2T}(\mathbf{r},t)$, that is

$$V_{(2T)}^{i}(\boldsymbol{r},t)=H\left[V_{2T}^{r}(\boldsymbol{r},t')\right], \tag{2.13b}$$

which is square integrable too. Hence we can now define the analytical signal $V_{2T}(\boldsymbol{r}, t)$ as follows

$$V_{2T}(\boldsymbol{r},t)=V_{2T}^{r}(\boldsymbol{r},t)+V_{(2T)}^{i}(\boldsymbol{r},t). \tag{2.13c}$$

The cross correlation of the analytical signals $V(\boldsymbol{r}_1, t)$ and $V(\boldsymbol{r}_2, t)$ is defined as

$$\left\langle V(\boldsymbol{r}_1,t+t)V^{*}(\boldsymbol{r}_2,t)\right\rangle=\lim_{T\to\infty}\frac{1}{2T}\int_{-\infty}^{\infty}V_{2T}(\boldsymbol{r}_1,t+t)V_{2T}^{*}(\boldsymbol{r}_2,t)\,dt, \tag{2.13}$$

where the function $V(\boldsymbol{r}, t)$ is the analytical signal associated to the function $V^{r}(\boldsymbol{r}, t)$. One important property of the cross correlation of two analytic signals is that the resultant function is again an analytical signal [14]. In consequence, all the necessary information of the Fourier transform is contained in the positive frequencies. In the next section we are going to define quantities related to the irradiance and the spectral irradiance.

2.4 **The Mutual Coherence Function and the Cross Spectral Density.**

In Radiometry, the irradiance is defined as the optical flux per unit area [watt/cm^2], and the spectral irradiance as flux per unit area per unit of wavelength [watt/cm^{2}nm]. These two radiometric quantities are

generalized in the Theory of Partial Coherence as the Mutual Coherence Function and the Cross Spectral Density, respectively.

The Mutual Coherence Function (of $V(\mathbf{r}, t)$) is defined as

$$G_{12}(t) = \left\langle V(\mathbf{r}_1, t+t) V^*(\mathbf{r}_2, t) \right\rangle, \tag{2.16}$$

where V is an analytical signal associated with a real function V^r that describes the optical field.

The Cross Spectral Density is defined as the Fourier transform respect to t of the Mutual Coherence Function, that is

$$W_{12}(w) = \begin{cases} \int_{-\infty}^{\infty} G_{12}(t) e^{iwt}\, dt & w > 0, \\ 0 & w < 0. \end{cases} \tag{2.17}$$

Note that $W_{12}(w)$ is equate to zero for $w<0$ since $W_{12}(w)$ is an analytic signal. The simplest example of a Cross Spectral Density is the one associated to an incoherent source. It is given by

$$W_{12}(w) = 2bE_I(w)d(\mathbf{r}_1 - \mathbf{r}_2), \tag{2.18}$$

where $E_I(w)$ is the spectral irradiance and b is a constant that allow $E_I(w)$ to retain the units of a spectral irradiance. In consequence the Mutual Coherence is the inverse Fourier transform with respect to w, denoted as $F^{-1}\{\}$, that is

$$\begin{aligned} G_{12}(t) &= F^{-1}\{2E_I(w)\}d(\mathbf{r}_1 - \mathbf{r}_2) \\ &= G(t)d(\mathbf{r}_1 - \mathbf{r}_2). \end{aligned} \tag{2.19}$$

where $G(t) = F^{-1}\{2E_I(w)\}$.

The definition of the Mutual Coherence given in Eq. (2.16) is valid only for sources that are stationary and ergodic[2]. A more general definition of the Mutual Coherence can be find in reference [14]. For our purposes the definition given in Eq. (2.16) is enough.

The irradiance of the optical field is obtained by evaluating the Mutual Coherence in the same point and for $t = 0$. In other words

$$G_{11}(0) = 2E(\mathbf{r}_1), \tag{2.20}$$

where we denote by E the irradiance distribution. In the same way, the spectral irradiance is obtained from Eq. (2.18), if we make $\boldsymbol{r}_1 = \boldsymbol{r}_2$, to give

$$W_{11}(w) = 2E_I(\boldsymbol{r}_1, w). \tag{2.21}$$

These particular examples of Cross Spectral Density and Mutual Coherence are used in the following chapters.

2.5. Summary of Symbols and Definitions.

In table 1 we display a summary of symbols, definitions and names to be used in this work. For the sake of completeness we add other definitions found in discussions of partial coherence theory.

[2] That a source is ergodic means that; the time average of a radiating entity of the source equals the ensamble

Table 1. Symbols and names used normally in Partial Coherence Theory.

Symbol	Name
$G_{12}(t) = G(\boldsymbol{r}_1, \boldsymbol{r}_2, t)$	Mutual Coherence Function.
$g_{12}(t) = \frac{G_{12}(t)}{\sqrt{G_{11}(0)}\sqrt{G_{22}(0)}}$	Complex Degree of Coherence.
$G_{11}(t) = G(\boldsymbol{r}_1, \boldsymbol{r}_1, t)$	Self-Coherence Function.
$G_{11}(0) = 2E(\boldsymbol{r}_1)$	Radiant Flux Density, or Irradiance.
$G_{12}(0) = J(\boldsymbol{r}_1, \boldsymbol{r}_2)$	Mutual Intensity Function.
$W_{12}(w) = W(\boldsymbol{r}_1, \boldsymbol{r}_2, w)$	1) Cross Spectral Density Function. 2) Mutual Power Spectrum. 3) Cross Power Spectrum.
$2E_l(\boldsymbol{r}, w) = W(\boldsymbol{r}, \boldsymbol{r}, w)$	Spectral Radiant Flux Density.

In the next chapter we will discuss the propagation of the Cross Spectral Density.

average of the source.

CHAPTER 3

Free space propagation of the cross spectral density.

3.1 Free space propagation of $G_{12}(t)$.

In this section we introduce the wave equation governing the propagation of the mutual coherence function $G_{12}(t)$.

We start assuming that the function $V^r(\boldsymbol{r}, t)$ represents an optical field, which satisfies the wave equation[3]

$$\nabla^2 V^r(\boldsymbol{r},t) = \frac{1}{c^2}\frac{\partial^2 V^r(\boldsymbol{r},t)}{\partial t^2}. \tag{3.1}$$

The analytic signal $V(\boldsymbol{r}, t) = V^r(\boldsymbol{r}, t) + iV^i(\boldsymbol{r}, t)$ also satisfies the wave equation, Eq. (3.1), since $V(\boldsymbol{r}, t)$ is a linear combination of two solutions. Then

$$\nabla^2 V(\boldsymbol{r},t) = \frac{1}{c^2}\frac{\partial^2 V(\boldsymbol{r},t)}{\partial t^2}. \tag{3.2}$$

We show next that the Mutual Coherence satisfies the wave equation, too. Let us suppose that the mutual coherence is given by (see Eq. (2.16))

$$G_{12}(t) = \langle V(\boldsymbol{r}_1, t+t)V^*(\boldsymbol{r}_2, t)\rangle, \tag{3.3}$$

where V is an analytic signal associated with a specific optical field. Then, we take the Laplacian with respect to the point $\boldsymbol{r}_1$ of the mutual coherence function $G_{12}(t)$, that is

$$\begin{aligned}\nabla_1^2 G_{12}(t) &= \nabla_1^2 \langle V(\boldsymbol{r}_1, t+t)V^*(\boldsymbol{r}_2, t)\rangle \\ &= \langle V^*(\boldsymbol{r}_2, t)\nabla_1^2 [V(\boldsymbol{r}_1, t+t)]\rangle.\end{aligned} \tag{3.4}$$

From Eq. (3.2) we obtain that

[3] Although the units system is irrelevant for the present work, we mention that all radiometric measurements

$$\nabla_1^2 V(\boldsymbol{r}_1, t+t) = \frac{1}{c^2}\frac{\partial^2 V(\boldsymbol{r}_1, t+t)}{\partial(t+t)} = \frac{1}{c^2}\frac{\partial^2 V(\boldsymbol{r}_1, t+t)}{\partial t^2}. \tag{3.5}$$

Substituting Eq. (3.5) in Eq. (3.4) we have

$$\begin{aligned}\nabla_1^2 G_{12}(t) &= \left\langle \left[\frac{1}{c^2}\frac{\partial^2 V(\boldsymbol{r}_1, t+t)}{\partial t^2}\right] V^*(\boldsymbol{r}_2, t)\right\rangle, \\ &= \frac{1}{c^2}\frac{\partial^2}{\partial t^2}\left\langle V(\boldsymbol{r}_1, t+t) V^*(\boldsymbol{r}_2, t)\right\rangle, \\ &= \frac{1}{c^2}\frac{\partial^2}{\partial t^2} G_{12}(t).\end{aligned} \tag{3.6}$$

On the other hand, if we apply the Laplacian with respect to $\boldsymbol{r}_2$, we obtain

$$\begin{aligned}\nabla_2^2 G_{12}(t) &= \nabla_2^2\left\langle V(\boldsymbol{r}_1, t+t) V^*(\boldsymbol{r}_2, t)\right\rangle, \\ &= \left\langle V(\boldsymbol{r}_1, t+t)\nabla_2^2 V(\boldsymbol{r}_2, t)\right\rangle, \\ &= \left\langle V(\boldsymbol{r}_1, t+t)\frac{1}{c^2}\frac{\partial^2 V(\boldsymbol{r}_2, t)}{\partial t^2}\right\rangle, \\ &= \lim_{T\to\infty}\frac{1}{2T}\int_{-\infty}^{\infty} V_{2T}(\boldsymbol{r}_1, t+t)\frac{1}{c^2}\frac{\partial^2 V_{2T}^*(\boldsymbol{r}_2, t)}{\partial t^2} dt.\end{aligned} \tag{3.7}$$

made in CENAM are related to the SI (MKS).

Integrating by parts the integral in Eq. (3.7), it follows that

$$\nabla_2^2 G_{12}(t) = \lim_{T\to\infty}\frac{1}{2T}V(\boldsymbol{r}_1,t+t)\frac{\partial V^*(\boldsymbol{r}_2,t)}{c^2\partial t}\bigg|_{-T}^{T} - \lim_{T\to\infty}\frac{1}{T}\frac{\partial V(\boldsymbol{r}_1,t+t)}{c^2\partial t}V^*(\boldsymbol{r}_2,t)\bigg|_{-T}^{T}$$

$$+\lim_{T\to\infty}\frac{1}{2T}\int_{-\infty}^{\infty}\frac{\partial^2 V_{2T}(\boldsymbol{r}_1,t+t)}{c^2\partial t^2}V_{2T}^*(\boldsymbol{r}_2,t)dt\,. \tag{3.8}$$

Considering that both V and its derivative are finites, the two first limits tend to zero. Therefore we obtain

$$\nabla_2^2 G_{12}(t) = \left\langle \frac{\partial^2 V(\boldsymbol{r}_1,t+t)}{c^2\partial t^2}V^*(\boldsymbol{r}_2,t)\right\rangle. \tag{3.9}$$

Since

$$\frac{\partial^2 V(\boldsymbol{r}_1,t+t)}{c^2\partial t^2} = \frac{\partial^2 V(\boldsymbol{r}_1,t+t)}{c^2\partial t'^2}, \tag{3.10}$$

then we have

$$\nabla_2^2 G_{12}(t) = \left\langle \frac{\partial^2 V(\mathbf{r}_1, t+t)}{c^2 \partial t^2} V^*(\mathbf{r}_2, t) \right\rangle,$$

$$= \frac{1}{c^2} \frac{\partial^2}{\partial t^2} G_{12}(t). \tag{3.11}$$

Summarizing, we have that

$$\nabla_S^2 G_{12}(t) = \frac{1}{c^2} \frac{\partial^2}{\partial t^2} G_{12}(t), \tag{3.12}$$

where *s* is a subindex that takes the value 1 or 2. This demonstrates that $G_{12}(t)$ is a solution of the wave equation. In other words, the mutual coherence of an optical field propagates identically as a wave. And given a mutual coherence function of an optical field, we can know the new mutual coherence function after a displacement of the optical field.

We can write the complete equation as

$$\nabla_1^2 \nabla_2^2 G_{12}(t) = \frac{1}{c^4} \frac{\partial^4}{\partial t^4} G_{12}(t). \tag{3.13}$$

3.2. **Wave Equation solution in terms of $W_{12}(w)$.**

It is straightforward to obtain the solution of Eq. (3.12) if we work with the Fourier time transform of $G_{12}(t)$, that is $W_{12}(w)$.

Let $W_{12}(w)$ be the Fourier time transform of $G_{12}(t)$. Since $G_{12}(t)$ is an analytic signal we have

$$G_{12}(t) = \frac{1}{2p}\int_0^\infty W_{12}(w)\,e^{iwt}\,dw\,. \tag{3.14}$$

Substituting Eq. (3.14) in Eq. (3.12), we obtain

$$\frac{1}{2p}\int_0^\infty \left[\nabla_s^2 + k^2(w)\right] W_{12}(w)\,e^{iwt}\,dw = 0\,, \tag{3.15}$$

where $k(w) = \dfrac{w}{c}$.

Since Eq. (3.15) must hold for all t, we have

$$\left[\nabla_s^2 + k^2(w)\right] W_{12}(w) = 0 \,. \tag{3.16}$$

Thus, we see that the cross-spectral density satisfies the Helmholtz equation. It is known that Eq. (3.16) with $s = 1$ has the formal solution [14]

$$W'(P_1, S_2, w) = -\int_{S_1} W(S_1, S_2, w) \frac{\partial G_1(P_1, P_1', w)}{\partial n_{S_1}}\bigg|_{P_1'=S_1} dS_1 \,, \tag{3.17}$$

where n_{s1} is the normal to the surface of integration. And $\dfrac{\partial}{\partial n_{s_1}}$ is the partial derivative with respect to the normal. Here G_1 is a Green's function satisfying the equation

$$\left[\nabla_s^2 + k^2(w)\right] G_1(P_1, P_1', w) = -d(P_1 - P_1'), \tag{3.18}$$

with the boundary condition,

$$G_1(P_1, P_1', w)\big|_{P_1'=S_1} = 0 \,. \tag{3.19}$$

In the same way, the solution for *s*=2 can be written as

$$W'(P_1,P_2,w)=\int_{S_2} W(P_1,S_2,w)\left.\frac{\partial G_2(P_2,P_2',w)}{\partial n_{S_2}}\right|_{P_2'=S_2} dS_2\ , \tag{3.20}$$

where G_2 is a Green's function satisfying the same boundary condition as G_1. Combining Eqs. (3.17) and (3.20) we obtain

$$W'(P_1,P_2,w)=\int_{S_2}\int_{S_1} W(S_1,S_2,w)\frac{\partial G_1}{\partial n_{S_1}}\frac{\partial G_2}{\partial n_{S_{"2}}}dS_1 dS_2\ . \tag{3.21}$$

Thus $W'(P_1,P_2,w)$ is obtained formally in terms of $W(S_1,S_2,w)$.

3.3. **Cross-Spectral density from a plane source.**

The Eq. (3.21) takes a particular form for planar sources. Let us suppose that we have a finite plane source *s*, on the system X´-Y´ at z = 0. The source has a cross-spectral density given by $W(S_1,S_2,w)$ (S_1 and S_2 are vectors) inside the source, and 0 outside it, see Fig. 3.1.

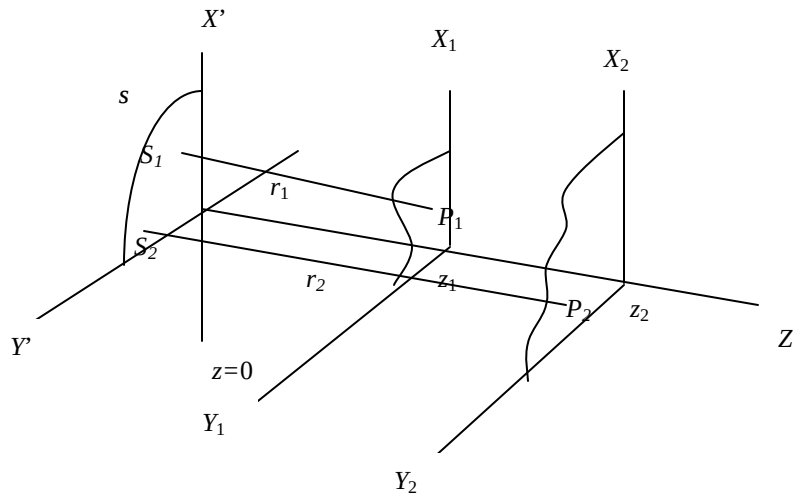

Fig. 3.1. Notation used in the Green´s functions.

The optical field propagates along the z-axis. And we want to obtain the cross spectral density at the points P_1 and P_2. They are at the planes z_1 and z_2 respectively. The distance P_1-S_1 is denoted as r_1, and the distance P_2-S_2 is denoted as r_2.

The Green´s functions G_1 and G_2 that satisfy the boundary conditions (at the source) are respectively,

$$G_1 = \frac{e^{ikr_1}}{4\pi r_1} - \frac{e^{ikr_1''}}{4\pi r_1''}, \tag{3.22}$$

and

$$G_2 = \frac{e^{ikr_2}}{4pr_2} - \frac{e^{ikr_2''}}{4pr_2''}, \tag{3.23}$$

where r_1'' and r_2'' are the distances to the mirror points of r_1 and r_2, respectively. That is

$$r_1 = \sqrt{(z_1 - z_1')^2 + (x_1 - x_2')^2 + (y_1 - y_2')^2}\,, \tag{3.24}$$

$$r_1'' = \sqrt{(z_1 + z_1')^2 + (x_1 - x_2')^2 + (y_1 - y_2')^2}\,. \tag{3.25}$$

And in the same manner for r_2 and r"$_2$.

The normal derivative of G is

$$\frac{\partial G_1}{\partial n_{S_1}} = \frac{(1 - ikr_1)}{4p}\frac{e^{ikr_1}}{r_1^2}\frac{\partial r_1}{\partial n_{S_1}} + \frac{(1 - ikr_1'')}{4p}\frac{e^{ikr_1''}}{r_1''^2}\frac{\partial r_1''}{\partial n_{S_1}}, \tag{3.26}$$

and

$$\left.\frac{\partial r_1}{\partial n_{S_1}}\right|_{S_1} = -\left.\frac{\partial r_1}{\partial z_1'}\right|_{S_1} = \frac{z_1}{r_1} = \left.\frac{\partial r_1''}{\partial z_1'}\right|_{S_1}. \tag{3.27}$$

Thus, if we define $\cos(q_1) = \frac{z_1}{r_1}$, we find that

$$\left.\frac{\partial G_1}{\partial n_{S_1}}\right|_{S_1} = -2\frac{1-ikr_1}{4p}\cos(q_1)\frac{e^{ikr_1}}{r_1^2}. \tag{3.28}$$

In the same manner, we obtain

$$\left.\frac{\partial G_2}{\partial n_{S_2}}\right|_{S_2} = -2\frac{1+ikr_2}{4p}\cos(q_2)\frac{e^{-ikr_2}}{r_2^2}. \tag{3.29}$$

Substituting Eq. (3.28) and Eq. (3.29) into Eq. (3.21) yields,

$$W'(P_1,P_2,w) = \frac{1}{4p^2}\int_{S_2}\int_{S_1} W(S_1,S_2,w)(1-ikr_1)(1+ikr_2)\cos(q_1)\cos(q_2)\frac{e^{ik(r_1-r_2)}}{r_1^2 r_2^2}dS_1 dS_2 . \tag{3.30}$$

We now use the approximation (1-*ikr*) ≅ -*ikr* for r much longer than the wavelength of radiation l, obtaining finally the next relation

$$W'(P_1,P_2,w)=\frac{1}{l^2}\int_{S_2}\int_{S_1}W(S_1,S_2,w)\cos(q_1)\cos(q_2)\frac{e^{ik(r_1-r_2)}}{r_1 r_2}dS_1 dS_2 . \qquad (3.31)$$

We arrive to the final Eq. (3.31), which describes the free propagation of the cross spectral density. In the next section we will apply this equation in two successive propagations to obtain the diffraction equation in terms of the Cross Spectral Density.

3.4 **Diffraction Equation in terms of $W_{12}(w)$.**

As was shown in the previous section, we have in Eq. (3.31) a mathematical way to calculate the free propagation of the cross spectral density $W_{12}(w)$. In this work we analyze the problem of diffraction in the general case of partially coherent sources. To do so a diffraction equation relating the cross spectral density would be helpful. Such an equation has been already discussed by K. Mielenz [17]. We can obtain it by applying two times the propagation equation. Let us consider the optical setup of Fig. 3.2. Here we have a plane source s described by $W(P_1,P_2,w)$, where P_1 and P_2 are the vectors of two points at the plane of the source.

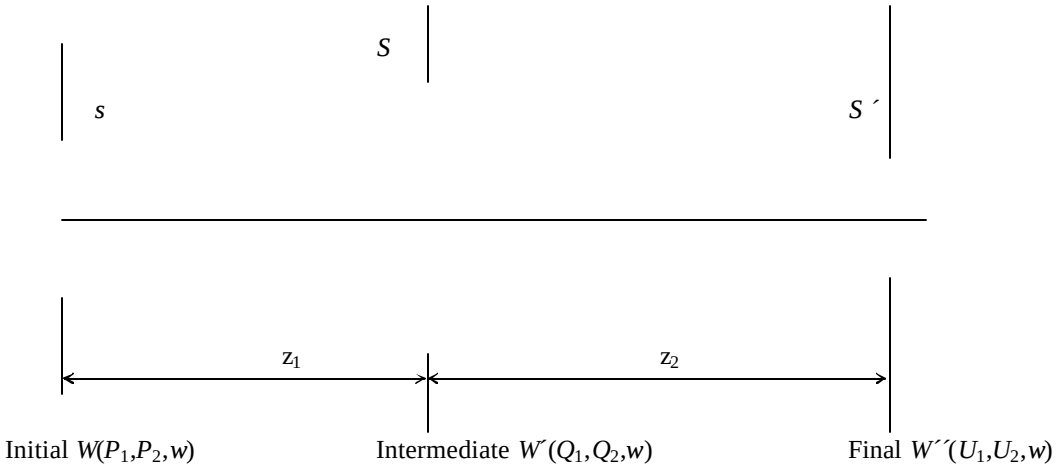

Fig. 3.2. Notation for the diffraction Equation. P_1 and P_2 are the vectors of two points at the source's plane. Q_1 and Q_2 are the vectors of two points at the plane of the aperture S. And U_1 and U_2 are the vectors of two points at the plane of the aperture $S\,´$.

In free propagation we can calculate $W´(Q_1,Q_2,w)$ in the aperture S by applying Eq. (3.31) as follows

$$W'(Q_1,Q_2,w)=\frac{1}{l^2}\int_{P_2}\int_{P_1}W(P_1,P_2,w)\cos(q_1)\cos(q_2)\frac{e^{ik(P_1Q_1-P_2Q_2)}}{P_1Q_1P_2Q_2}dP_1dP_2\,. \qquad (3.32)$$

If we apply once again Eq. (3.31) using Eq. (3.32) to calculate $W´´(U_1,U_2,w)$, we have

$$W''(U_1,U_2,w)=\frac{1}{l^4}\int_{Q_2}\int_{Q_1}\int_{P_2}\int_{P_1} W(P_1,P_2,w)\cos(q_1)\cos(q_2)\cos(q_1')\cos(q_2') \frac{e^{ik(P_1Q_1-P_2Q_2)}}{P_1Q_1\cdot P_2Q_2}\frac{e^{ik(Q_1U_1-Q_2U_2)}}{Q_1U_1\cdot Q_2U_2}dP_1dP_2dQ_1dQ_2 \quad (3.33)$$

Eq. (3.33) describes the relationship between the final cross spectral density, *W´´*, in terms of the initial cross spectral density, *W*; through an integral transform. This is the basic relationship that is used in this thesis.

CHAPTER 4

Cross Spectral Density propagated through a Circular Aperture.

We are interested in calculating the irradiance distribution produced by two successive apertures. The apertures are circular and with different diameters. They are concentric respect to the propagation axis. In metrology it is common to assume that the source is spatially incoherent, polychromatic, and it has a circular shape. For the sake of simplicity, here we restrict our numerical results to monochromatic sources.

We begin by assuming that the first illuminated aperture is a partially coherent source, which is described by its respective cross spectral density. The next aperture is then a diffracting aperture. Our task is to find the correspondent cross spectral density behind the diffracting aperture.

Previous work in this direction is obviously the expression that describes the diffraction produced by a circular aperture illuminated with a point source; as given by Lommel [18] and independently by H. Struve [18]. For the case of an extended incoherent source the superposition principle in intensity is used. The total intensity is obtained integrating over the entire source. These two cases must be cover by our generalization. We start this chapter by giving the expressions of these two cases. The cases of a circular aperture, illuminated by a point source and illuminated by a extended source, serve as a benchmark (or reference frame) to compare our result.

4.1. Illumination with a monochromatic point source.

In the past century E. Lommel, and independently H. Struve, reported the diffraction pattern produced by a circular aperture when it is illuminated by a point source [18]. Lommel and Struve were interested in evaluating the out-of-focus images of a monochromatic point source. The knowledge of the Fresnel distribution near focus was of particular importance for estimating the tolerances when setting the observation plane in an image forming system. In particular, Lommel presented a solution in terms of infinite series.

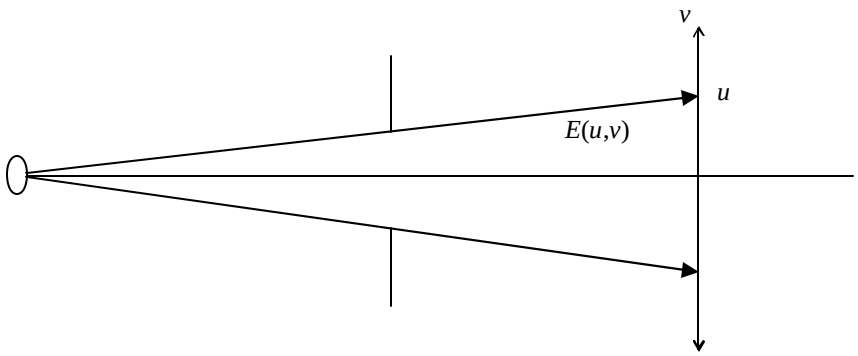

Fig. 4.0. Optical Arrangement showing the notation used in the Fresnel diffraction.

The irradiance distribution was described as

$$E(u,v) = E_0\left[C^2(u,v) + S^2(u,v)\right], \tag{4.1}$$

where the variable u is a geometrical parameter related to the system. And it gives the radio (in dimensionless units) of the geometrical projection of the aperture, see Fig 4.0. The variable v is a normalized radial distance from the center of the diffraction pattern. The constant E_0 is the irradiance at the origin and the functions $C(u,v)$ and $S(u,v)$ are the real and imaginary parts of the Fresnel integral in polar coordinates. These functions have the next solutions

$$\begin{aligned} \mathrm{C}(u,v) &= \frac{2}{u}\left[\frac{2}{u}\sin\left(\frac{v^2}{2u}\right)+\sin\left(\frac{u}{2}\right)\mathrm{V}_0(u,v)-\cos\left(\frac{u}{2}\right)\mathrm{V}_1(u,v)\right] \qquad \text{for } v<u, \\ &= \frac{2}{u}\left[\cos\left(\frac{u}{2}\right)\mathrm{U}_1(u,v)+\sin\left(\frac{u}{2}\right)\mathrm{U}_2(u,v)\right] \qquad \text{for } v>u, \end{aligned} \tag{4.2}$$

and

$$\begin{aligned} \mathrm{S}(u,v) &= \frac{2}{u}\left[\cos\left(\frac{v^2}{2u}\right)-\cos\left(\frac{u}{2}\right)\mathrm{V}_0(u,v)-\sin\left(\frac{u}{2}\right)\mathrm{V}_1(u,v)\right] \qquad \text{for } v<u, \\ &= \frac{2}{u}\left[\sin\left(\frac{u}{2}\right)\mathrm{U}_1(u,v)-\cos\left(\frac{u}{2}\right)\mathrm{U}_2(u,v)\right] \qquad \text{for } v>u, \end{aligned} \tag{4.3}$$

where $\mathrm{V}_0(u,v)$, $\mathrm{V}_1(u,v)$, $\mathrm{U}_1(u,v)$ and $\mathrm{U}_2(u,v)$ are the Lommel functions [19]; which he developed for this purpose. These functions are defined as

$$U_n(u,v)=\sum_{s=0}^{\infty}(-1)^s\left(\frac{u}{v}\right)^{n+2s}J_{n+2s}(v), \tag{4.4}$$

and

$$V_n = \sum_{s=0}^{\infty} (-1)^s \left(\frac{v}{u} \right)^{n+2s} J_{n+2s}(v), \tag{4.5}$$

where *n* is the index of the Lommel function and *s* is the index of the series. These functions are complicate to evaluate. In fact, their convergence is slow for large values of *u*. This is the reason why some authors developed axintotic approximations. Nevertheless, the recent development of powerful personal computers, together with efficient mathematical software makes it possible to evaluate the Lommel functions.

In the case of an extended incoherent source, the irradiance distribution is calculated by using the superposition principle. The resulting expression is

$$E(u,v) = \int_S E_S(\vec{v}_S) \left[C^2(u, \vec{v} - \vec{v}_S) + S^2(u, \vec{v} - \vec{v}_S) \right] v_S \, dv_S \, dg \ , \tag{4.6}$$

where the integration is performed over the surface of the source. (v_s, g) are polar coordinates at the plane of the source.

We note that, the expression given in Eq. (4.6) is a particular case of a more general problem. The general problem is the diffraction pattern of a circular aperture, illuminated by a partially coherent source. The solution to this general problem is the subject of the rest of the present chapter, and it constitutes one of

the interesting contributions of this work. In the next section we switch from the concept of irradiance to the concept of cross spectral density.

4.2. Cross Spectral Density propagated through a Circular Aperture (in the Fresnel Approximation).

The setup to be analyzed is shown in Fig. 4.1, where we have a Radiometric Bench consisting of a thermal source followed by two limiting apertures *s* and *S*, and a detector.

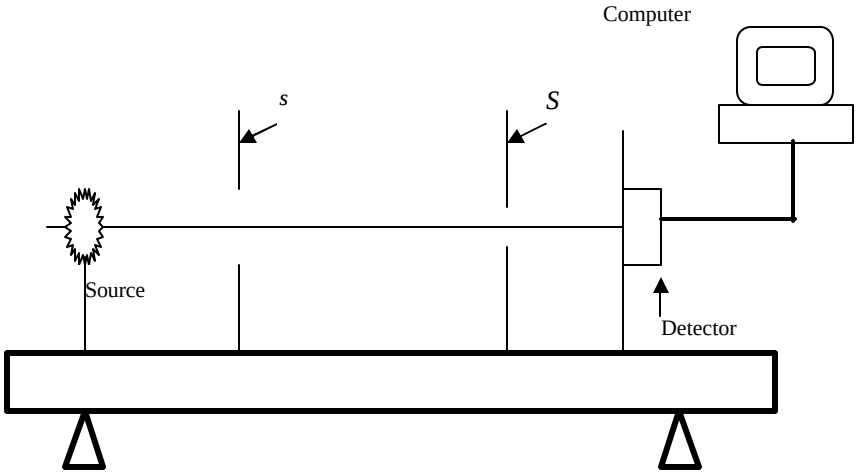

Fig. 4.1. Radiometric bench.

The main idea of our proposal is that the aperture *s* can be thought of as a secondary partially coherent source with a cross spectral density denoted as $W(P_1,P_2,w)$, which can be easily calculated by using the van Cittert-Zernike theorem [20]. The aperture *S* is acting as a diffracting aperture, and the plane of the detector is the observation plane. As mentioned before we are interested to find the cross spectral density, $W''(U_1,U_2,w)$,

in the plane of the detector. The irradiance distribution can be obtained by setting the cross spectral density at the same point. That is $E(U)=(1/2)W''(U,U,w)$.

The notation used in this work is shown schematically in Fig. 4.2, where the scheme shows a circular geometry with its respective polar coordinates. In our setup s represents a circular aperture of radius a, placed in front of an incoherent source, the radiation that passes through the aperture s illuminates other circular aperture of radius R, denoted by S. This second aperture is placed at a distance z_1 in front of s. Finally, S' represents the active area of the detector with radius c, placed at a distance z_2 from the circular aperture S.

Let us choose two arbitrary points P_1 and P_2 over the aperture s, with coordinates (x_1,y_1) and (x_2,y_2) respectively. These points have also polar coordinates (l_1, f_1) and (l_2, f_2). In the same way, we denote two arbitrary points in the aperture S by $Q_1(x_1,h_1)$ and $Q_2(x_2,h_2)$ with polar coordinates (Rr_1, a_1) and (Rr_2, a_2) respectively; where r_i is a dimensionless parameter that varies between 0 and 1. Finally, let us consider two arbitrary points in the aperture S' given by $U_1(s_1,h_1)$ and $U_2(s_2,h_2)$, with polar coordinates (r_1,b_1) and (r_2,b_2). We denote by R_1, R_2, R'_1 and R'_2, the distances between each pair of points P_1Q_1, P_2Q_2, Q_1U_1 and Q_2U_2 respectively.

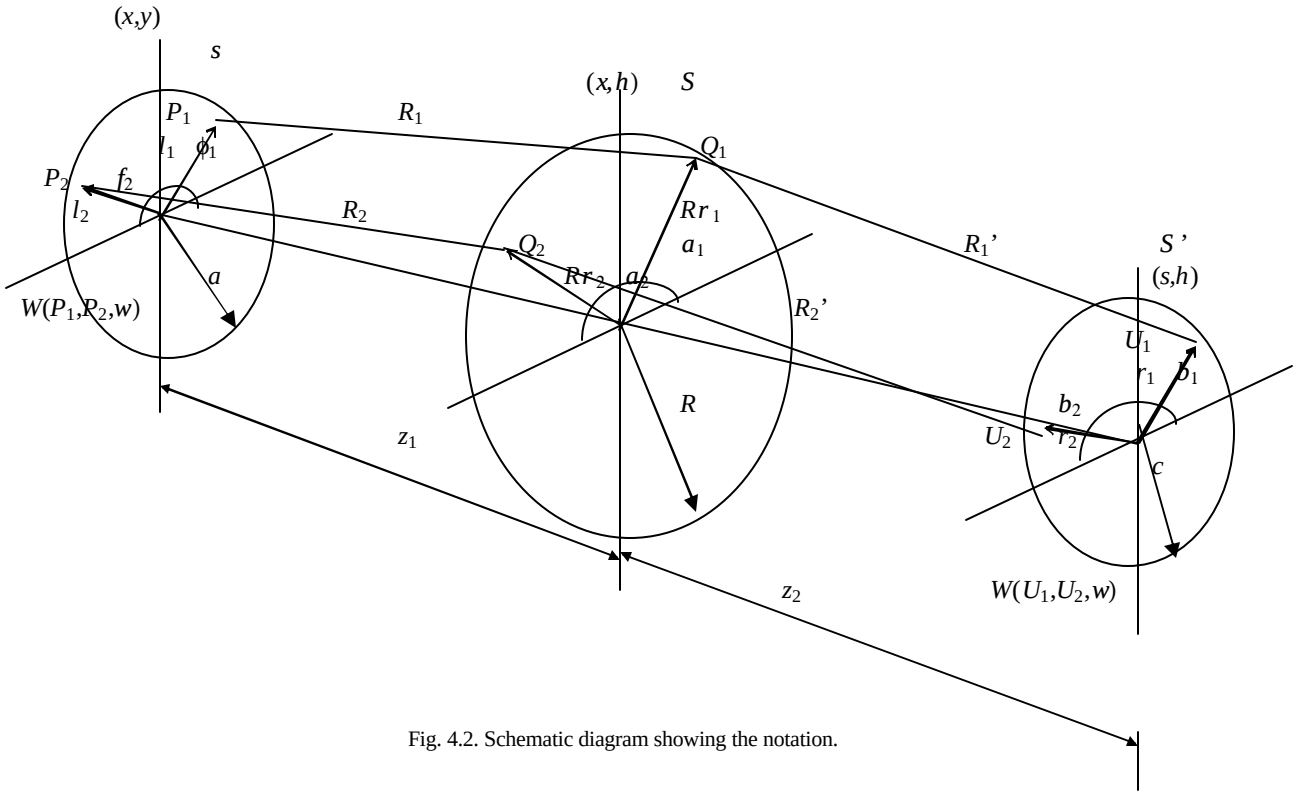

Fig. 4.2. Schematic diagram showing the notation.

The equation that relates the cross spectral density, $W''(U_1,U_2,w)$, in the plane of the detector with the cross spectral density, $W(P_1,P_2,w)$, in the plane of the aperture s was discussed in chapter 3, and it is given by Eq. (3.31). In order to perform our calculation, we rewrite Eq. (3.31) using the new notation; namely

$$W''(U_1,U_2,w)=\frac{1}{l^4}\int_{Q_2}\int_{Q_1}\int_{P_2}\int_{P_1}\frac{\cos(\boldsymbol{n},\boldsymbol{Q_1U_1})\cos(\boldsymbol{n},\boldsymbol{Q_2U_2})}{R_1'R_2'}\frac{\cos(\boldsymbol{n},\boldsymbol{P_1Q_1})\cos(\boldsymbol{n},\boldsymbol{P_2Q_2})}{R_1R_2}$$

$$W(P_1,P_2,w)e^{ik[R_1-R_2+R_1'-R_2']}dP_1dP_2dQ_1dQ_2 \quad , \tag{4.7}$$

where as indicated before the function $W(P_1,P_2,w)$ is the cross spectral density at the aperture s, the function $\cos(\boldsymbol{n}, \boldsymbol{P_iQ_i})$ (with i = 1, 2) is the cosine of the angle between the vector $\boldsymbol{P_iQ_i}$ and the normal $\boldsymbol{n}$ in the point P_i. The same description applies for $\cos(\boldsymbol{n}, \boldsymbol{Q_iU_i})$.

Next, we make a simplification of Eq. (4.7) by assuming the following geometrical approximations:

$$\cos(\boldsymbol{n},\boldsymbol{P_1Q_1}) \approx \cos q_1, \tag{4.8.1}$$

$$\cos(\boldsymbol{n},\boldsymbol{P_2Q_2}) \approx \cos q_2, \tag{4.8.2}$$

$$\cos(\boldsymbol{n},\boldsymbol{Q_1U_1}) \approx \cos q'_1, \tag{4.8.3}$$

$$\cos(\boldsymbol{n},\boldsymbol{Q_2U_2}) \approx \cos q'_2, \tag{4.8.4}$$

where q_1 and q_2 are the angles between the optical axis and the vectors $\boldsymbol{O_sQ_1}$ and $\boldsymbol{O_sQ_2}$ respectively (see fig.4. 3). The same geometry applies for the angles q'_1 and q'_2, with vectors that can be formed between O_SU_1 and O_SU_2.

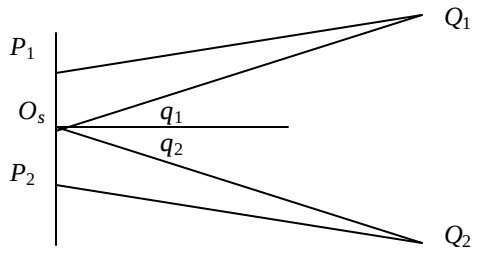

Fig. 4.3. Approximation of the angle $(\boldsymbol{n}, \boldsymbol{P_1Q_1})$ by q_1, $(\boldsymbol{n}, \boldsymbol{P_2Q_2})$ by q_2, etc.

Even more, we consider these four cosines approximately equal to unity, as was taken in the paraxial approximation. Using this, we can reduce the last equation as follows

$$W''(U_1,U_2,w)=\frac{1}{l^4}\int_{Q_2}\int_{Q_1}\int_{P_2}\int_{P_1}\frac{1}{R_1'R_2'}\frac{1}{R_1R_2} W(P_1,P_2,w)e^{ik[R_1-R_2+R_1'-R_2']}dP_1dP_2dQ_1dQ_2 \quad . \tag{4.9}$$

Now, in the same manner as the developed used in the Fresnel approximation, we can estimate the distances R_1-R_2 and R'_1-R'_2 as

$$R_1-R_2 \cong \frac{1}{2z_1}\left[(x_1-x_1)^2+(h_1-y_1)^2-(x_2-x_2)^2-(h_2-y_2)^2\right], \tag{4.10.1}$$

$$R_1'-R_2' \cong \frac{1}{2z_2}\left[(x_1-s_1)^2+(h_1-h_1)^2-(x_2-s_2)^2-(h_2-h_2)^2\right]. \tag{4.10.2}$$

And the products R_1R_2 and $R'_1R'_2$ can be expressed as

$$R_1R_2 \cong z_1^2 \text{ and } R'_1R'_2 \cong z_2^2. \tag{4.10.3}$$

Consequently, we have that

$$R_1 - R_2 + R_1' - R_2' = \frac{1}{2}\left(\frac{z_1 + z_2}{z_1 z_2}\right)\left[x_1^{\,2} + h_1^{\,2} - x_2^{\,2} - h_2^{\,2}\right] + \frac{1}{2z_1}\left[x_1^2 + y_1^2 - x_2^2 - y_2^2\right]$$
$$+ \frac{1}{2z_2}\left[s_1^2 + h_1^2 - s_2^2 - h_2^2\right] + \left(\frac{x_2}{z_1} + \frac{s_2}{z_2}\right)x_2 + \left(\frac{y_2}{z_1} + \frac{h_2}{z_2}\right)h_2$$
$$- \left(\frac{x_1}{z_1} + \frac{s_1}{z_2}\right)x_1 - \left(\frac{y_1}{z_1} + \frac{h_1}{z_2}\right)h_1 \quad . \tag{4.11}$$

Hence, by substituting Eq. (4.11) into Eq. (4.9) and rearranging terms, the expression for $W''(U_1, U_2, \omega)$ results in

$$W''(U_1, U_2, w) = \frac{e^{i\frac{k}{2z_2}\left[s_1^2 + h_1^2 - s_2^2 - h_2^2\right]}}{l^4 z_1^{\,2} z_2^{\,2}} \int_{Q_2}\int_{Q_1}\int_{P_2}\int_{P_1} W(P_1, P_2, w)\, e^{i\frac{k}{2}\left[\frac{z_1 + z_2}{z_1 z_2}\right]\left(x_1^{\,2} + h_1^{\,2} - x_2^{\,2} - h_2^{\,2}\right)}$$
$$e^{i\frac{k}{2z_1}\left(x_1^2 + y_1^2 - x_2^2 - y_2^2\right)}$$
$$e^{ik\left[\left(\frac{x_2}{z_1} + \frac{s_2}{z_2}\right)x_2 + \left(\frac{y_2}{z_1} + \frac{h_2}{z_2}\right)h_2 - \left(\frac{x_1}{z_1} + \frac{s_1}{z_2}\right)x_1 - \left(\frac{y_1}{z_1} + \frac{h_1}{z_2}\right)h_1\right]}$$
$$dP_1 dP_2 dQ_1 dQ_2 \quad . \tag{4.12}$$

Eq. (4.12) is the Fresnel approximation of Eq. (4.7). The integrals with respect to Q_1 and Q_2 are easy to evaluate, if we employ cylindrical coordinates. With this goal in mind, let us change to polar coordinates by using the following transformations

$$\begin{aligned} x_j &= l_j \cos f_j , \\ y_j &= l_j \sin f_j , \qquad j=1,\ 2, \end{aligned} \tag{4.13.1}$$

$$\begin{aligned} x_j &= R r_j \cos a_j , \\ h_j &= R r_j \sin a_j , \qquad j=1,\ 2, \end{aligned} \tag{4.13.2}$$

$$\begin{aligned} s_j &= r_j \cos b_j , \\ h_j &= r_j \sin b_j , \qquad j=1,\ 2, \end{aligned} \tag{4.13.3}$$

where the notation was explained previously, see Fig. 4.2.

If we use Eqs. (4.13.1) to (4.13.3) then we can rewrite the two initial terms of the sum (within the second exponential in the integrand) as follows

$$k\left[\left(\frac{x_2}{z_1}+\frac{s_2}{z_2}\right)x_2+\left(\frac{y_2}{z_1}+\frac{h_2}{z_2}\right)h_2\right]=$$
$$\left(\frac{l_2\cos f_2}{z_1}+\frac{r_2\cos b_2}{z_2}\right)kRr_2\cos a_2+\left(\frac{l_2\sin f_2}{z_1}+\frac{r_2\sin b_2}{z_2}\right)kRr_2\sin a_2=$$
$$\left(\frac{kRl_2\cos f_2}{z_1}+\frac{kRr_2\cos b_2}{z_2}\right)r_2\cos a_2+\left(\frac{kRl_2\sin f_2}{z_1}+\frac{kRr_2\sin b_2}{z_2}\right)r_2\sin a_2 \quad . \tag{4.14}$$

In a similar manner we can write the relationship for the coordinates with subindex 1. By substituting the expressions for the coordinates with subindex 1 and with subindex 2, in Eq. (4.12), we have

$$W''(U_1,U_2,w)=\frac{R^4}{l^4z_1^2z_2^2}e^{i\frac{k}{2z_2}\left[r_1^2-r_2^2\right]}\int_{Q_2}\int_{Q_1}\int_{P_2}\int_{P_1}W(P_1,P_2,w)e^{i\frac{kR^2}{2}\left[\frac{z_1+z_2}{z_1z_2}\right]\left(r_1^2-r_2^2\right)}e^{i\frac{k}{2z_1}\left(l_1^2-l_2^2\right)}$$
$$e^{i\left[\left(\frac{kRl_2}{z_1}\cos f_2+\frac{kRr_2}{z_2}\cos b_2\right)r_2\cos a_2+\left(\frac{kRl_2}{z_1}\operatorname{sen} f_2+\frac{kRr_2}{z_2}\operatorname{sen} b_2\right)r_2\operatorname{sen} a_2\right]}$$
$$e^{-i\left[\left(\frac{kRl_1}{z_1}\cos f_1+\frac{kRr_1}{z_2}\cos b_1\right)r_1\cos a_1+\left(\frac{kRl_1}{z_1}\operatorname{sen} f_1+\frac{kRr_1}{z_2}\operatorname{sen} b_1\right)r_1\operatorname{sen} a_1\right]}$$
$$l_1df_1l_2df_2dl_1dl_2r_1r_2da_1da_2dr_1dr_2 \quad . \tag{4.15}$$

Now, it is helpful to use the next normalized coordinates

$$u=k\frac{z_1+z_2}{z_1z_2}R^2, \tag{4.16.1}$$

$$v_j = k\frac{R}{z_2}r_j, \quad j = 1, 2, \tag{4.16.2}$$

$$l'_j = \frac{kRl_j}{z_1}, \quad j = 1, 2. \tag{4.16.3}$$

If we substitute them in Eq. (4.15) we obtain

$$W''(U_1,U_2,w) = \frac{R^4}{l^4 z_1^2 z_2^2} e^{i\frac{z_2}{2R^2k}\left[v_1^2 - v_2^2\right]} \int_{Q_2}\int_{Q_1}\int_{P_2}\int_{P_1} W(P_1,P_2,w) e^{i\frac{u}{2}\left(r_1^2 - r_2^2\right)} e^{i\frac{z_1}{2R^2k}\left(l_1'^2 - l_2'^2\right)}$$

$$e^{i\left[\left(l'_2\cos f_2 + v_2\cos b_2\right)r_2\cos a_2 + \left(l'_2\sin f_2 + v_2\sin b_2\right)r_2\sin a_2\right]}$$

$$e^{-i\left[\left(l'_1\cos f_2 + v_1\cos b_1\right)r_1\cos a_1 + \left(l'_1\sin f_2 + v_1\sin b_1\right)r_1\sin a_1\right]}$$

$$\left(\frac{z_1}{kR}\right)^4 l'_1 df_1 l'_2 df_2 dl'_1 dl'_2 r_1 r_2 da_1 da_2 dr_1 dr_2 \ . \tag{4.17}$$

We continue by considering the next change of variables; let us define L and Y new polar coordinates, given as

$$
\begin{aligned}
L_1 \cos\Psi_1 &= l_1' \cos f_1 + v_1 \cos b_1, \\
L_1 \sin\Psi_1 &= l_1' \sin f_1 + v_1 \sin b_1, \\
L_2 \cos\Psi_2 &= l_2' \cos f_2 + v_2 \cos b_2, \\
L_2 \sin\Psi_2 &= l_2' \sin f_2 + v_2 \sin b_2.
\end{aligned}
\tag{4.18}
$$

The respective Jacobians are given as

$$
\begin{aligned}
J_1 &= \frac{L_1}{\left[L_1^2 + v_1^2 - 2L_1 v_1 \cos(Y_1 - b_1)\right]^{1/2}}, \\
J_2 &= \frac{L_2}{\left[L_2^2 + v_2^2 - 2L_2 v_2 \cos(Y_2 - b_2)\right]^{1/2}}.
\end{aligned}
\tag{4.19}
$$

From the transformations in Eq. (4.18), we obtain for l'_1 and l'_2 the identities

$$
\begin{aligned}
l_1' &= \left[L_1^2 + v_1^2 - 2L_1 v_1 \cos(Y_1 - b_1)\right]^{1/2}, \\
l_2' &= \left[L_2^2 + v_2^2 - 2L_2 v_2 \cos(Y_2 - b_2)\right]^{1/2}.
\end{aligned}
\tag{4.20}
$$

By substituting Eqs. (4.18), (4.19) and (4.20) in Eq. (4.17) we obtain

$$W''(U_1,U_2,w)=\frac{R^4}{l^4 z_1^2 z_2^2}\left(\frac{z_1}{kR}\right)^4 e^{i\frac{z_2}{2R^2k}\left(v_1^2-v_2^2\right)}\int_{Q_2}\int_{Q_1}\int_{P_2'}\int_{P_1'}W\left(P_1',P_2',w\right)e^{i\frac{u}{2}\left(r_1^2-r_2^2\right)}$$
$$e^{i\frac{z_1}{2R^2k}\left(L_1^2+v_1^2-2L_1v_1\cos(Y_1-b_1)-L_2^2-v_2^2+2L_2v_2\cos(Y_2-b_2)\right)}$$
$$e^{i[L_2\cos(Y_2)r_2\cos(a_2)+L_2\sin(Y_2)r_2\cos(a_2)]}$$
$$e^{-i[L_1\cos(Y_1)r_1\cos(a_1)+L_1\sin(Y_1)r_1\cos(a_1)]}$$
$$\frac{L_1}{l_1'}l_1'df_1\frac{L_2}{l_2'}l_2'df_2dL_1dL_2r_1r_2da_1da_2dr_1dr_2\quad,$$

(4.21)

where the point $P\ell_j$ represents the point P_j, but now given in terms of the new coordinates L_j y Y_j.

With the help of the Bessel functions [21] we can integrate Eq. (4.21) with respect to a_1 and a_2 to obtain

$$W''(U_1,U_2,w)=\frac{1}{(2p)^4}\frac{z_2^2}{z_1^2}e^{i\frac{z_2}{2R^2k}\left(v_1^2-v_2^2\right)}\int_{Q_2}\int_{Q_1}\int_{P_2'}\int_{P_1'}W\left(P_1',P_2',w\right)e^{i\frac{u}{2}\left(r_1^2-r_2^2\right)}e^{i\frac{z_1}{2R^2k}\left(L_1^2-L_2^2\right)}e^{i\frac{z_1}{2R^2k}\left(v_1^2-v_2^2\right)}$$
$$e^{i\frac{z_1}{R^2k}(L_2v_2\cos(Y_2-b_2)-L_1v_1\cos(Y_1-b_1))}$$
$$e^{i[L_2r_2\cos(a_2-Y_2)]}$$
$$e^{-i[L_1r_1\cos(a_1-Y_1)]}$$
$$L_1dY_1L_2dY_2dL_1dL_2r_1r_2da_1da_2dr_1dr_2\quad,$$

$$W''(U_1,U_2,w)=\frac{1}{(2p)^4}\frac{z_2^2}{z_1^2}e^{i\frac{z_1+z_2}{2R^2k}\left(v_1^2-v_2^2\right)}\int_{P_2'}\int_{P_1'}W\left(P_1',P_2',w\right)e^{i\frac{z_1}{2R^2k}\left(L_1^2-L_2^2\right)}e^{i\frac{z_1}{R^2k}\left(L_2v_2\cos(Y_2-b_2)-L_1v_1\cos(Y_1-b_1)\right)}$$
$$\int_{Q_2}\int_{Q_1}e^{i\frac{u}{2}\left(r_1^2-r_2^2\right)}e^{i[L_2r_2\cos(a_2-Y_2)]}e^{-i[L_1r_1\cos(a_1-Y_1)]}$$
$$r_1r_2da_1da_2dr_1dr_2L_1dY_1L_2dY_2dL_1dL_2\ .$$

(4.22)

The integrals with respect to r_j (j=1,2) in Eq. (4.22) have a known solution in terms of Lommel functions. Let us denote by C(u,v) and S(u,v) the real and imaginary part of the integral

$$2\int_0^1 J_0\left(Lr_j\right)e^{-i\frac{u}{2}r_j^2}r_j dr_j=C(u,L)-iS(u,L)\ . \tag{4.23}$$

The functions C and S are the same defined in Eq. (4.1); and their solutions are given in Eq. (4.2) and Eq. (4.3). By using Eq. (4.23) in Eq. (4.22) we have finally that

$$W''(U_1,U_2,w)=\frac{1}{(2p)^4}\frac{z_2^2}{z_1^2}e^{i\frac{z_1+z_2}{2R^2k}\left(v_1^2-v_2^2\right)}\int_{P_2'}\int_{P_1'}W\left(P_1',P_2',w\right)e^{i\frac{z_1}{2R^2k}\left(L_1^2-L_2^2\right)}e^{i\frac{z_1}{R^2k}\left(L_2v_2\cos(Y_2-b_2)-L_1v_1\cos(Y_1-b_1)\right)}$$
$$p^2\left[C(u,L_2)-iS(u,L_2)\right]\left[C(u,L_1)+iS(u,L_1)\right]$$
$$L_1dY_1L_2dY_2dL_1dL_2\ ,$$

(4.24)

where as mentioned above the notation $W(P'_1,P'_2,w)$ means that the function W is given in terms of the new variables of integration. Eq. (4.24) gives the cross spectral density in a plane behind the diffracting aperture in terms of the cross spectral density of the illuminating source. As an important particular case, with this relation we obtain straightforward the diffraction of this circular aperture for the general case, where it is illuminated by a partially coherent source.

The demonstration that Eq. (4.24) contains two particular cases: the diffraction pattern due to a point source, and that due to an extended, circular, incoherent source. These two cases are discussed in chapter 5. Here we conclude that the general expression, given in Eq. (4.24) describes the cross spectral density propagated through a circular aperture.

Next, we address a subtle problem arising when we make the change of variables, in Eq. (4.18). Care must be taken to use the right integration limits. Basically there are two conditions. The first condition is when $v<a'$, where $a'=kRa/z_1$, and the second when $v \geq a'$. The first case is depicted in Fig.4.4. In the scheme we show the source with a normalized radio a', which in the new coordinate system is centered at the point v (without loss of generality we have selected the angular coordinate $b = 0$).

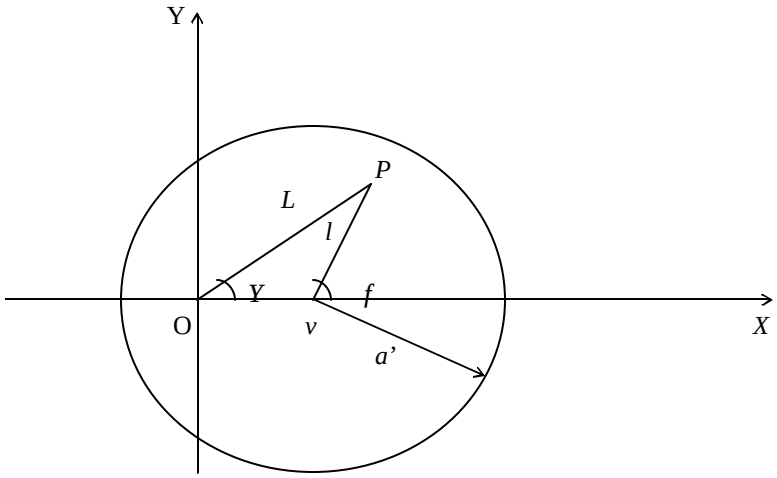

Fig. 4.4. Schematic representation of the integration area.

A point P in the source has the polar coordinates (l, f) respect to the old coordinate system (x, y). In the new system it has the coordinates (L, Y). We must integrate then over the enter circle of radio a' centered at v. We see that Y varies between 0 and $2p$, and the variation of L is a function of Y. It is easy to show that any point P' along the edge of the source has a radial coordinate given as

$$L(Y) = v\cos(Y) + \left[v^2\cos^2(Y) - v^2 + a'^2\right]^{1/2}. \tag{4.25}$$

The second case is depicted in Fig. 4.5, where now $v \geq a'$. In this case we see that Y varies between two maxima values.

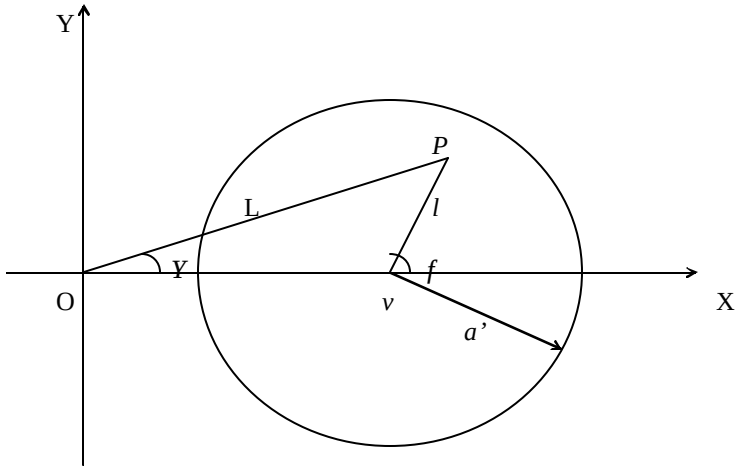

Fig. 4.5. Schematic representation of the integration area, case $v \geq a'$.

Let us denote by Y_0 the maximum value of Y, which is reached when the vector $\boldsymbol{L}$ is tangent to the circumference of the source. Such a maximum is shown in Fig. 4.6.

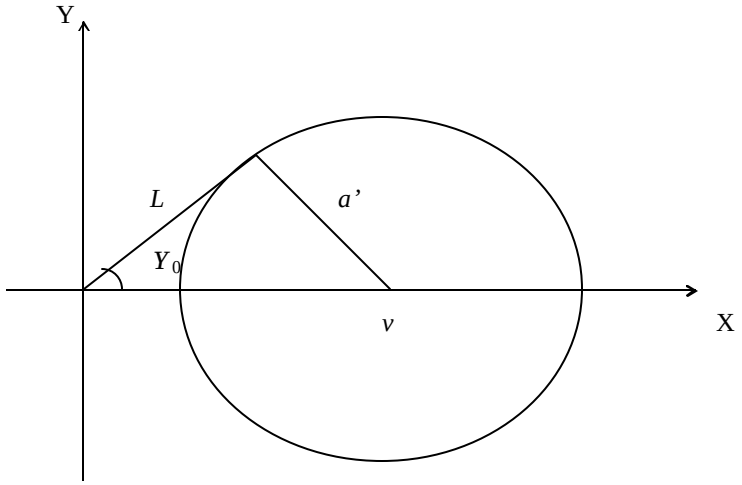

Fig. 4.6. Maximum value Y_0. The variable Y can take values between Y_0 and $-Y_0$.

The maxima and minima limits of Y are $Y_{0,}$ and $-Y_0$ respectively. From Fig. 4.6 is it easy to deduce that Y_0 is given as

$$Y_0 = \arcsin\left(\frac{a'}{v}\right). \tag{4.26}$$

Once again L is function of Y, and given a constant Y' we can define a minimum $L_0(Y')$ and a maximum $L_f(Y')$ as depicted in Fig. 4.7.

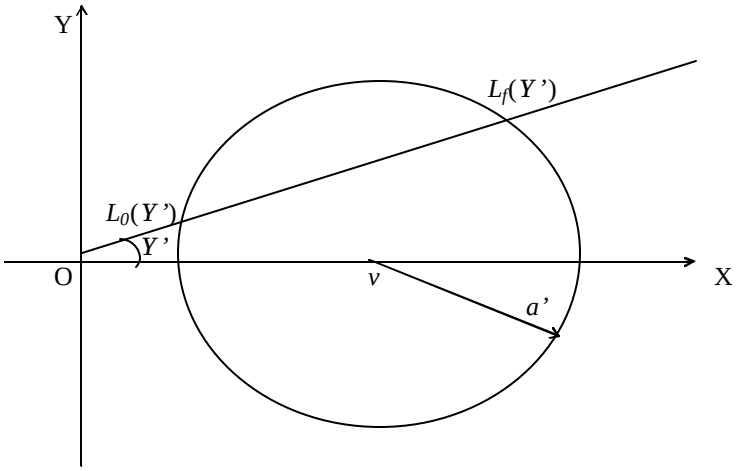

Fig. 4.7. Possible values of L for a given Y'.

From Fig. 4.7 we see that any value of $L(Y)$ always lies between these two limits. With the help of a simple calculus we can deduce the next relations for the two limits $L_0(Y')$ and $L_f(Y')$,

$$L_0(Y') = \frac{1}{\cos Y'} \frac{v - \left(v^2 - \left(1+\tan^2 Y'\right)\left(v^2 - a'^2\right)\right)^{1/2}}{1+\tan^2 Y'} \quad ,$$
$$L_f(Y') = \frac{1}{\cos Y'} \frac{v + \left(v^2 - \left(1+\tan^2 Y'\right)\left(v^2 - a'^2\right)\right)^{1/2}}{\left(1+\tan^2 Y'\right)} \quad . \tag{4.27}$$

The relations given in (4.27), (4.26) and (4.25) can be used in any numerical simulation of Eq. (4.24). The use of these relations increments the efficiency of the algorithm. In the next section we return to Eq. (4.24) to discuss some important properties of the transmission function of the system.

4.3. Transmission Function.

We can associate to any imaging system (in the more general concept) a transmission function [22] denoted by $K(U_i, P_i, \omega)$ which describes the system's response evaluated at the point U_i in the image plane, due to a point source situated at P_i. In such a way that the image of an extended object can be constructed by means of the transfer function with the relation

$$W''(U_1,U_2,w) = \iint W(P_1,P_2,w) K(U_1,P_1,w) K^*(U_2,P_2,w) dP_1 dP_2 \, , \tag{4.28}$$

where $W''(U_1,U_2,w)$ and $W(P_1,P_2,w)$ are the cross spectral densities of the image and the object respectively. Obviously the function $K(U_i, P_i, \omega)$ depends of the geometry of the system. In case of our system we can deduce the functional form of such a function by simple comparing Eq. (4.28) with our general solution given in Eq. (4.24).

From the comparison between both equations we obtain for the transmission function the relationship

$$K(\mathrm{l}', f; \mathrm{v}, b) = -\frac{1}{i l'^2 z_1 z_2}\left(\frac{\mathrm{z}_1}{\mathrm{k}}\right)^2 \mathrm{e}^{\mathrm{i}\frac{z_1+z_2}{2R^2\mathrm{k}}\mathrm{v}^2}\ \mathrm{e}^{\mathrm{i}\frac{z_1}{R^2\mathrm{k}}\left[\frac{L^2}{2} - \mathrm{Lv}\cos(Y-b)\right]}\left[C(\mathrm{u},\mathrm{L}) - \mathrm{i}S(\mathrm{u},\mathrm{L})\right], \tag{4.29}$$

where L is given by

$$L = \left[l'^2 + v^2 + 2l'v\cos(f-b)\right]^{1/2}. \tag{4.30}$$

Here Eq. (4.30) is obtained directly from Eq. (4.18). We describe next some features of the transmission function given in Eq. (4.29). We notice that it is proportional to the complex amplitude of the Fresnel diffraction due to a circular aperture and illuminated by a point source. We see, too, that this complex amplitude is a function of the projected distance in the image plane between a point P of the source and a point U in the image plane. The last is easy to demonstrate with the help of Eq. (4.30), where we have that L is the projected distance between the points P and U. The transmission function depends also of the square of

the projected distance L^2, and of the product Lv. We can conclude here that since the transmission function $K(U, P, w)$ is not a function only of the projected distance $K(U-P, w)$, the condition of isoplanatic region is not satisfied.

As a complementary analysis we can obtain the transmission function in the Fraunhofer approximation. If we approximate the exponentials in Eq. (4.22) to unity, then we obtain the far field approximation, that is

$$\mathrm{W}(U_1, U_2, w) = \frac{1}{(2p)^4}\left(\frac{z_1}{z_2}\right)^2 \int_{P_2'}\int_{P_1'} W(P_1', P_2', w)\frac{\mathrm{J}_1(L_1)}{L_1}\frac{\mathrm{J}_1(-L_2)}{L_2}{}_2\, L_1 \mathrm{d}L_1\, \mathrm{d}Y_1\, L_2 \mathrm{d}L_2\, \mathrm{d}Y_2 \quad . \tag{4.31}$$

It follows then that the transmission function is given as

$$K(\mathrm{l}', f; \mathrm{v}, b) = \frac{z_1}{(2p)^2 z_2}\frac{\mathrm{J}_1(L)}{L} \, . \tag{4.32}$$

In this case we see that the transmission function depends only of the projected distance L. Therefore, in this case the isopanatic region condition is satisfied. We have here in polar coordinates the equivalent case to that given by Mielenz in rectangular coordinates, Eq. (12) in reference [23].

4.4 Numerical Simulation.

The practical application of Eq. (4.24) can be demonstrated with the next numerical example. Here we want to see if the aperture s (which is always two or more times bigger than aperture S) can contribute significantly in the final diffraction at the image plane or if its effect is negligible [24]. A common practice in radiometry is to use s as an aperture that limits the stray light. And the aperture S is used to limit the radiation to be measured. In such a system the aperture s must be bigger than the aperture S .

Such effects are of practical importance in the calculation of the diffraction errors (1-f_1) and (1-f_2), where the functions f_1 and f_2 are the quotient of the total flux that falls on the detector (when there is an aperture) divided by the total flux that falls when there is not an aperture [6]. These functions are given as

$$f_1 = \frac{1}{2}\int_0^{a+c} D(v,a,c)E(u,v)v\,dv\,, \tag{4.33}$$

and

$$f_2 = \frac{1}{2}\left(\frac{u}{c}\right)^2 \int_0^{a+c} D(v,a,c)E(u,v)v\,dv\,, \tag{4.34}$$

where the function $D(v, a, c)$ is a convolution of the circles of the source of radio a and of the detector of radio c (see appendix A). And the function $E(u, v)$ is the expression of the diffraction produced by the circular aperture and a point source, Eq. (4.1). These two formulations were deduced using Eq. (4.6), which is the expression for an extended incoherent circular source.

The effect of a second aperture is usually neglected arguing that the contribution to the diffraction error is small compared to the effect of the first one. However there were no any direct way to evaluate how small it really is. With the formalism described by Eq. (4.24) we can take into account in a direct way the effect of the presence of this second aperture. We show next some numerical calculations where we show that the presence of the second aperture can become important, at least as a modification in the irradiance profile. In order to see the effect of the use of a second aperture in Radiance Measurements (aperture s in Fig. 4.1), we have calculated the irradiance distribution in the plane of the detector for three different cases. In the first case we considered a point source and only one aperture, that is the aperture S. In the second case we considered an expanded incoherent source and the aperture S. And in the last case we considered the same expanded incoherent source but now with both apertures (s and S). For these calculations we considered a circular incoherent source of radio a_0=0,3mm, an aperture s of radio a=4mm, and an aperture S of radio R=1,06mm. The distance between the source and the aperture s is z_0=1m, the distance between the apertures s and S is z_1=1m, and finally the distance between the aperture S and the plane of the detector is z_2=0,5m. The present configuration corresponds to a value of u in Eq.(4.16.1) equal to u=28,9306. The evaluation was done by using the correspondent expressions given in Eq. (4.1), Eq. (4.6) and Eq. (4.24). In the third case, the Cross Spectral Density in the aperture s is given as

$$W(P_1, P_2, w) = \frac{E_S}{z_0^2} \frac{2J_1(d)}{d} \exp[ij], \tag{4.35}$$

where

$$d = \frac{z_1 a_0}{z_0 R}\sqrt{L_1^2 + L_2^2 - 2L_1 L_2 \cos\left(\Psi_1 - \Psi_2\right)}, \tag{4.36a}$$

and

$$j = \frac{z_1^2}{2 z_0 k R^2}\left[L_1^2 - L_2^2 - 2L_1 v\cos\left(\Psi_1\right) + 2L_2 v\cos\left(\Psi_2\right)\right], \tag{4.36b}$$

and we have approximate the exponential term to unity. We show in Fig. 4.8 the irradiance profiles obtained numerically; Fig. 4.8*A* represents the irradiance at the detector plane for the case 1, Fig. 4.8*B* corresponds to the case 2, and finally Fig. 4.8*C* represents the case 3.

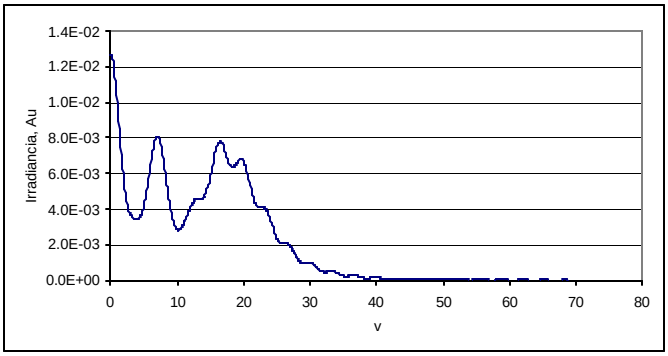

Fig. 4.8*A*. Irradiance distribution due to a point source, u=28,9360.

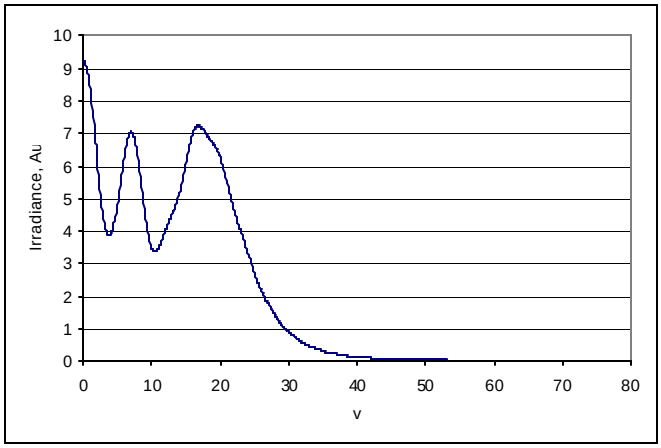

Fig. 4.8*B*. Irradiance distribution due to an extended incoherent source, u=28,9360.

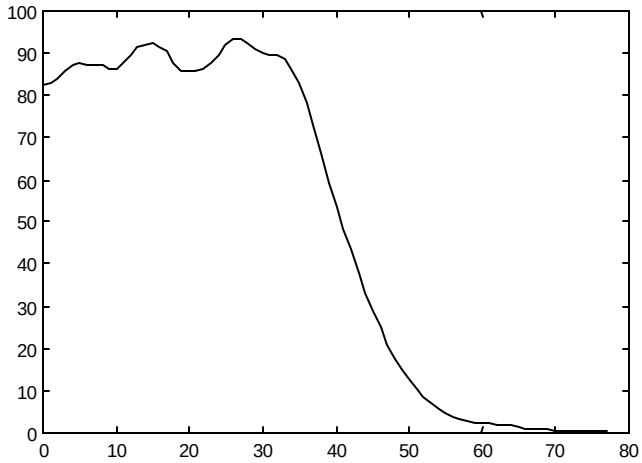

Fig. 4.8*C*. Irradiance distribution due to the same extended incoherent source and two apertures, u=28,9360.

We see that the difference between considering a point source and an extended source is only an effect of smoothing (see graphics 4.8*A* and 4.8*B*). Whereas the use of a second intermediate aperture (aperture *s*) can produce significant secondary diffraction effects. This situation is clear if we compare the graphic in Fig. 4.8*C* with the diffraction produced by a point source located in the center of the plane of the aperture *s*. Such diffraction is shown in Fig. 4.9. We can see a coincidence between the three secondary maximum (before *v*=35) of Fig. 4.8*C* and the three maximum of Fig. 4.9. We can say then that, despite that the aperture *s* is 4 times bigger than the aperture *S*, it can affect strongly in the calculation of diffraction errors. It is clear from our results that the use of a second aperture could modify significantly the irradiance distribution at the detector's plane. In consequence, the use of an accurate model of the irradiance due to two successive apertures is necessary. Such a model is given by Eq. (4.24). The exact evaluation of f_1 and f_2 is beyond the scope of this work.

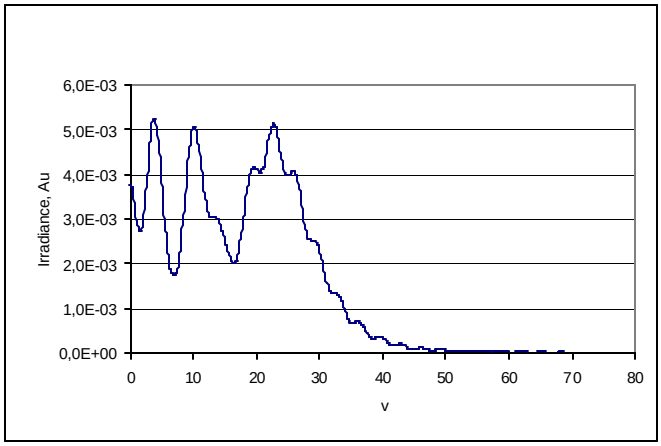

Fig. 4.9. Irradiance distribution due to a point source located in the plane of the aperture *s*, u=35,4.

In the next chapter we treat the limiting case where the secondary source s is an incoherent source. The importance of such case will be clear because the useful results obtained can be applied to reduce current calculations made in radiometry.

CHAPTER 5

Cross spectral density due to an incoherent source.

Here we analyze the limiting case where the aperture s is an incoherent source. For this case, we obtain the particular cross spectral density, from the general equation derived in chapter 4. We emphasize that the cross spectral density here obtained contains free-space propagation and near-field diffraction by aperture S; whereas the van Cittert-Zernike theorem only consider free propagation (see for example reference [15]). The diffracted field is the one due to the diffraction with a circular aperture. In the development of this theme, it will be necessary to define a Dirac delta function in terms of the variables L and Y. It is the subject of the next section.

5.1. Representation of an incoherent source in polar coordinates.

It is well-known that, the diffraction pattern produced by a circular aperture illuminated by an incoherent source. It is given by Eq. (4.6). But up to our knowledge, no body has published expressions of the cross spectral density for such an optical setup. The cross spectral density is useful for evaluating multiple

successive apertures. We can obtain this expression from the general equation (4.25). To do this, we employ the cross spectral density $W(P_1,P_2,w)$, over s, on polar coordinates (L,Y).

Let us consider the aperture s as an incoherent source. At the cross spectral density $W(P_1,P_2,w)$ (see Fig. 4.1) can be represented by a Dirac delta function as follows

$$W(P_1,P_2,w) = W(x_1, y_1, x_2, y_2, w) = E_l(w)d(x_1\text{-}x_2, y_1\text{-}y_2), \tag{5.1}$$

where $E_l(\omega)$ is the spectral exitance of the source, defined in Eq. (2.21). The Dirac delta function of Eq. (5.1) is given in rectangular coordinates. And as mentioned above, we need to represent it in the displaced polar coordinates. We can start with an expression given in reference [25] where the author discusses the Dirac delta function in ordinary polar coordinates. It is given as follows

$$d(\vec{r} - \vec{r}_0) = \frac{1}{r}d(r - r_0)d(f - f_0). \tag{5.2}$$

If we apply this definition to Eq. (5.1) we obtain

$$W(P_1, P_2, w) = E_l(w)\frac{1}{l_2'}d(l_2' - l_1')d(f_2 - f_1). \tag{5.3}$$

Apart of constants, which we do not discuss in this work. Eq. (5.3) represents the cross spectral density of an incoherent source in polar coordinates.

Next, we require to express the Dirac delta function in terms of the proposed variables L and Y. This in the sense that both functions must reproduce the same values, that is, infinite when $l'_2=l'_1$ and $f_2=f_1$. And zero in any other case. Let us see what values take L_2 and Y_2 when $l'_2=l'_1$ and $f_2=f_1$.

From Eq. (4.19) we substitute $l'_2 = l'_1$ and $f_2 = f_1$ to obtain

$$\begin{aligned} L_1\cos\Psi_1 &= l_1'\cos f_1 + v_1\cos b_1, \\ L_1\sin\Psi_1 &= l_1'\sin f_1 + v_1\sin b_1, \\ L_2\cos\Psi_2 &= l_1'\cos f_1 + v_2\cos b_2, \\ L_2\sin\Psi_2 &= l_1'\sin f_1 + v_2\sin b_2. \end{aligned} \tag{5.4}$$

Adding and subtracting $v_1\cos b_1$ and $v_1\sin b_1$ at the two last identities in the transformation (5.3), we have

$$\begin{aligned} L_2\cos\Psi_2 &= l_1'\cos f_1 + v_1\cos b_1 - v_1\cos b_1 + v_2\cos b_2, \\ L_2\sin\Psi_2 &= l_1'\sin f_1 + v_1\sin b_1 - v_1\sin b_1 + v_2\sin b_2, \end{aligned} \tag{5.5}$$

or

$$\begin{aligned} L_2 \cos\Psi_2 &= L_1 \cos\Psi_1 - v_1 \cos b_1 + v_2 \cos b_2, \\ L_2 \sin\Psi_2 &= L_1 \sin\Psi_1 - v_1 \sin b_1 + v_2 \sin b_2. \end{aligned} \tag{5.6}$$

We denote as L'_1 and Y'_1 the particular values of L_2 and Y_2 when $l'_2 = l'_1$ and $f_2 = f_1$. From Eq. (5.6) it results that

$$L'_1 = \left[\left(L_1 \cos\Psi_1 - v_1 \cos b_1 + v_2 \cos b_2 \right)^2 + \left(L_1 \sin\Psi_1 - v_1 \sin b_1 + v_2 \sin b_2 \right)^2 \right]^{\frac{1}{2}}, \tag{5.7}$$

and

$$\Psi'_1 = arctan \frac{L_1 \sin\Psi_1 - v_1 \sin b_1 + v_2 \sin b_2}{L_1 \cos\Psi_1 - v_1 \cos b_1 + v_2 \cos b_2} \quad . \tag{5.8}$$

Using L_1' and Y_1' we propose to write an expression equivalent to Eq. (5.3) but in terms of L and Y as follows

$$W\left(P'_1, P'_2, w\right) = E_0(w) \frac{1}{L_2} d\left(L_2 - L'_1\right) d\left(\Psi_2 - \Psi'_1\right). \tag{5.9}$$

This equation is, apart of constants, the cross spectral density of an incoherent source in the displaced polar coordinates (L, Y). The validity of this expression becomes evident in the next section; where we use it to evaluate Eq. (4.25) for an incoherent illumination of the aperture s.

5.2 Cross Spectral Density due to an Incoherent Source.

We can proceed to obtain the cross spectral density $W''(U_1,U_2,w)$ of the diffracted field in the detector plane, see fig. 4.1, when the aperture s is an incoherent source. If we substitute the expression given in Eq. (5.9) in Eq. (4.25), then the cross spectral density is

$$W''(U_1,U_2,w)=\frac{p^2R^4}{l^4z_1^2z_2^2}\left(\frac{z_1}{kR}\right)^4 e^{i\frac{z_1+z_2}{2R^2k}\left(v_1^2-v_2^2\right)}$$
$$\iint_{P_2'P_1'} E_0(w)\frac{1}{L_2}d(L_2-L_1')d(Y_2-Y_1')\, e^{i\frac{z_1}{2R^2k}\left(L_1^2-L_2^2\right)}$$
$$e^{i\frac{z_1}{R^2k}\left(L_2v_2\cos(Y_2-b_2)-L_1v_1\cos(Y_1-b_1)\right)}\left[C(u,L_2)-iS(u,L_2)\right]\left[C(u,L_1)+iS(u,L_1)\right]$$
$$L_1dY_1L_2dYdL_1dL_2\ ,$$

(5.10a)

and solving the integral in the variables L_2 and Y_2, we obtain

$$W''(U_1,U_2,w)=\frac{p^2E_0(w)}{l^4z_1^2z_2^2}\left(\frac{z_1}{k}\right)^4 e^{i\frac{z_1+z_2}{2R^2k}\left(v_1^2-v_2^2\right)}\int_{P_1'} e^{i\frac{z_1}{2R^2k}\left(L_1^2-L_1'^2\right)} e^{i\frac{z_1}{R^2k}\left(L_1'v_2\cos(Y_1'-b_2)-L_1v_1\cos(Y_1-b_1)\right)} \left[C(u,L_1')-iS(u,L_1')\right]\left[C(u,L_1)+iS(u,L_1)\right] L_1\,dY_1\,dL_1\,, \tag{5.10b}$$

where L'_1 and Y'_1 are functions of L_1 and Y_1, see Eq. (5.9), Eq. (5.8) and Eq. (5.7). Eq. (5.10b) is our general expression for the cross spectral density $W''(U_1,U_2,w)$ obtained in the detector plane, if the aperture s is considered as an incoherent source. The four-fold integral reduces to a two-fold integral. Our expression permits us then to evaluate the cross spectral density in the Fresnel approximation of an optical field diffracted by a circular aperture illuminated by an incoherent source. In some sense, our Eq. (5.10) is the diffracting version of the van Citter-Zernik theorem. In fact, the last is contained in Eq. (5.10).

In many cases we are interested in the irradiance (or the spectral radiant flux density) of the optical field. The spectral irradiance of the present configuration is $E_l(U) = W(U, U, w)$. From Eq. (5.9) the spectral irradiance reduces to

$$E_l(U)=\frac{p^2E_0(w)}{l^4z_1^2z_2^2}\left(\frac{z_1}{k}\right)^4\int_L\int_Y\left[C^2(u,L)+S^2(u,L)\right]L\,dY\,dL\,. \tag{5.11}$$

The two exponentials in Eq. (5.10b) become unity and the obtained spectral irradiance due to an incoherent source depends only of the functions C(u,L) and S(u,L). Since it is only a double integral and the values of the functions C and S can be already disposed in an array or a vector, then Eq. (5.11) is easier to evaluate numerically. Apart of constants, Eq. (5.11) is a simplified version of Eq. (4.6). This shows the reproducibility of classical results [26]. In a numerical calculation the effort spend in evaluating Eq. (5.11) is

less than the effort evaluating Eq. (4.6). In the next section we present numerical simulations, and experimental results of several practical situations.

5.3. Numerical Example.

We calculated numerically Eq. (5.11) for three different examples. For that purpose we use a conventional PC using commercially available mathematical software. In each example the diameter of the aperture s is different. In the first case we have considered a normalized diameter a'=1, in arbitrary units. In the second example, we set a'=10. And finally for the third case we set a'=100. For these examples the geometrical parameter u in Eq. (4.16.1) is $250p$. We show in Fig. 5.1 normalized graphics of the examples.

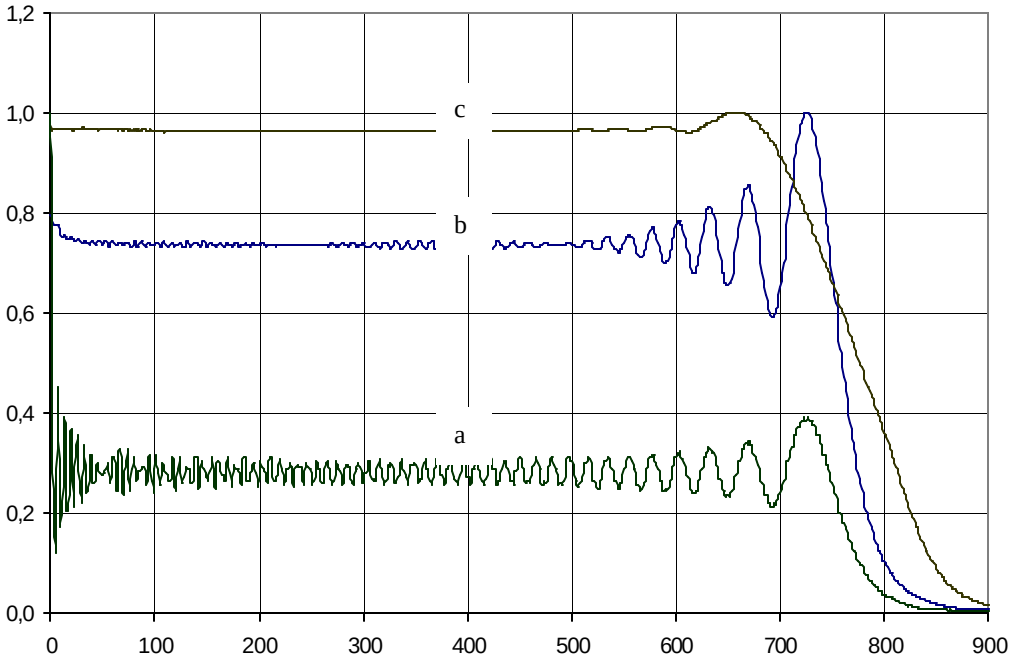

Fig. 5.1. Numerical evaluations of Eq. (5.11) for different aperture radios *a*': a) *a*'=1, b) *a*'=10, c) *a*'=100 and u=250π.

The curve labeled as a) belongs to *a*'=1, which is the one due to a point source. This numerical result is in perfect concordance with the experimental results reported by Boivin in 1975, see ref. [7]. In this paper, Boivin reports the measurement of the diffraction pattern of a system with the geometry above discribed. The curve labeled b) belongs to *a*'=10. We see in this graphic an effect of smoothing, except at the edge where diffraction appears stronger. Finally the curve c) belongs to *a*'=100. Here we can see that the diffraction effects are reduced and that the curve follows practically the geometric projection of the aperture. Since radiometric setups can fall in any of these three cases, it is evident the importance of making corrections with respect to the ideal geometric projection.

The Fresnel's integrals are normally known in rectangular coordinates. If we substitute the rectangular coordinates by polar coordinates for a problem with cylindrical symmetry, and solve the integrals, then we obtain a solution in terms of the Lommel's functions, Eq. (4.1). The Eq. (4.1) describes the diffraction pattern produced by an aperture illuminated by a point source. In the case of an extended source, the diffraction pattern is calculated by integrating the diffraction pattern produced by each point of the source, see Eq. (4.6). The Eq. (5.11) is the same as the Eq.(4.6), but given with different variables. Whereas normally the Eq.(4.6) is handle with the polar coordinates (l, f) (see fig.4.2), in Eq.(5.11) we handle it with new displaced polar coordinates (L, Y).

The advantage of handling the Eq. (5.11) with the displaced polar coordinates is that; apart of solve the Eq. (4.17) it offers an reduced way to calculate numerically the Eq. (5.11) (it also applies to Eq.(4.24)). For example, in the case of Eq. (4.6) we need to calculate for each pair of coordinates (l, f) the projected distance between a point U in the observation plane and a point S in the source (normally denoted as U-S). We see also that; the integration in the angular variable is performed always from 0 to $2p$. Whereas that, in the case of Eq. (5.11), for a given value of Y we know the initial and final values of L (see Fig. 4.4 and Fig. 4.5). Here it is important to note that, L is physically the distance U-S, as can be demonstrated from Eq. (4.30). Hence, we can give directly the values of L instead of calculate them. Also, the integration over the angular variable, in this case Y, we note that; the integration is not always performed from 0 to $2p$, as it is evident from Fig. 4.5 and Fig. 4.6.

We show in the next section a typical example of experimental results.

5.4. Experimental Results.

The service of radiance calibrations at CENAM is based on a radiance standard that consists in a tungsten lamp inside an integrating sphere, with stabilized flux. The radiance standard is calibrated periodically each year in order to conserve the trazability to National References. In the case of this instrument, the trazability is to the Primary Standard of the National Institute of Standards and Technology of U.S.A.

Actually at CENAM, a project to links the trazability of this instrument to National References of CENAM is developed. The project consist mainly of two parts; The first one is the preparation of an optical setup where the radiance standard is calibrated by measuring the radiant flux, that arrives into an absolute detector; in an optical configuration similar to the one shown in Fig. 4.1. And where the diffraction effects will be treated with the present work. The second part consists of the preparation of a detector as an absolute reference. It can be a calibrated detector or directly the Primary Standard of CENAM [27]; which was recently implemented at CENAM to be the basis of several radiometric measurements. The formalism proposed and developed in this thesis gives the tools to analyze and improve the measuring system.

A preliminary experiment was carried out using as source the radiance standard. The source was adjusted with a diameter of 0,5mm. A narrow band filter was used to obtain quasi-monochromatic light. The aperture S, placed at a distance z_1=1m has a diameter of 2,12mm, and the absolute detector was placed at a distance z_2 = 0,56m (see Fig. 4.1). This optical configuration corresponds to a value of u in Eq. (4.16.1) of 35,49.

We show in Fig. 5.2a the image of the irradiance that arrives to the detector. Fig. 5.2b shows the normalized profile of the image shown in Fig. 5.2a. The profile was obtained by directly scanning the photograph shown in Fig. 5.2a. The noise shown in the profile is mainly due to the scanning process.

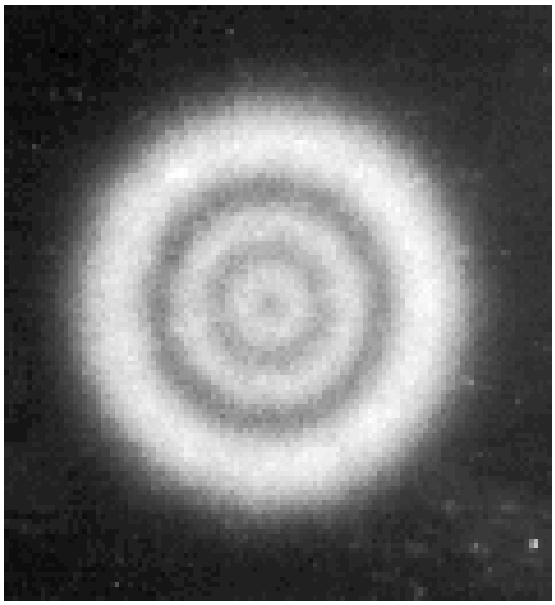

Fig. 5.2a. Experimental results for an expanded source of diameter 0.5 mm with z_1=1m, z_2=0.56m, an aperture diameter of 2.12mm and a wavelength of 550nm.

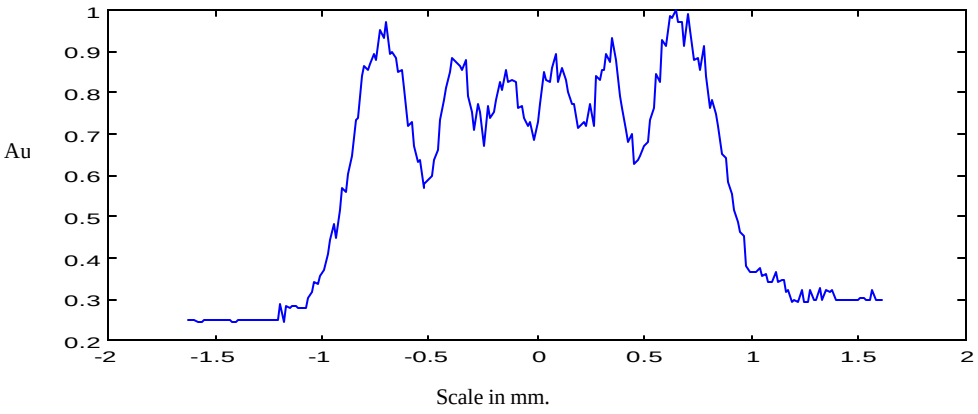

Fig. 5.2b. Normalized profile of the experimental irradiance distribution showing in Fig. 5.2a.

We perform next the numerical calculation of the irradiance for this experimental configuration using Eq. (5.11). We show in Fig. 5.2c the corresponding irradiance profile. Note that despite of the noise, both profiles are practically the same. The respective calculation of diffraction errors with Eqs. (4.33) and (4.34) (slightly modified to be used with our Eq. (5.11)) will permit links the trazability of the radiance standard with our National Primary Standard.

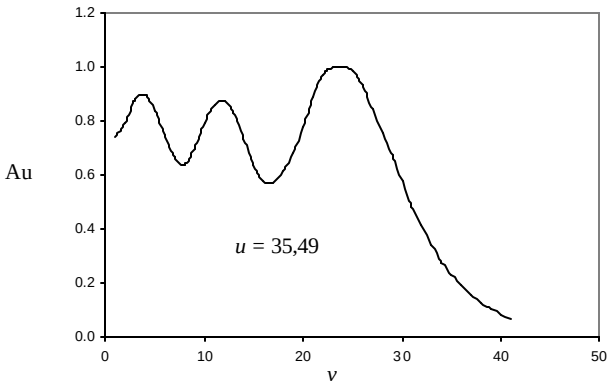

Fig. 5.2c. Numerical evaluation of Eq. (5.11) for the experimental parameters of Fig. 5.2a.

As we have shown, our simplified equation (5.11) reproduces quite well our experimental results. This is an experimental demonstration of the equivalence between our formalism and classical results given by Eq. (4.6). It is also a demonstration of the consistence of our analytic results.

CHAPTER 6

Conclusions.

In this work we have calculated the Cross Spectral Density propagated through a circular aperture in the Fresnel approximation. The obtained expression is a four-fold integral in terms of displaced polar coordinates. These introduced coordinates reduce the effort spend in numerical calculations and also they are convenient variables to work with general conditions of partial coherence.

We have obtained also the transmission functions of our system in the Fresnel as well as the Fraunhofer approximations. We note that, the transmission function obtained in this work takes into account the problem of no-isoplanatic region presented in the Fresnel approximation. In the case of the Fraunhofer approximation, the system is an isoplanatic imaging system.

We have used our general expression of the Cross Spectral density to demonstrate that the use of a second aperture, in radiometric measurements, can produce significant deviations of the currently used diffraction model, which is the basis for the calculations of corrections factors. Better analytic expressions for calculations of the correction factors can now be obtained using our general expression.

Also we have given the expression of the cross spectral density of an optical field diffracted by a circular aperture illuminated by an extended incoherent source. It can be compared, in a certain sense, with the van Cittert-Zernike Theorem where it gives the respective cross spectral density in free propagation of an optical field generated by an extended incoherent source.

Finally we have shown experimental results, which are according with our formalism.

CHAPTER 7

References.

[1] Sanders, C. L., and Jones, O. C., “nombre”. J. Opt. Soc. Am. **52**. 731 (1962).

[2] Blevin W. R., “Diffraction Losses in Radiometry and photometry”. Metrologia, **6**, 2, 39-44 (1970).

[3] L. P. Boivin. “Diffraction Losses Associated with Tungsten Lamps in Absolute Radiometry”. Applied Optics, **14**, 1, 197-200 (1975).

[4] Ooba, N., “nombre”. J. Opt. Soc. Am. **54**. 357 (1964).

[5] Focke J., “Total Ilumination in an aberration-free diffraction image”. Optica Acta. **3**, 4, 161-163 (1956).

[6] Steel W. H., De M., and Bell J. A., “Diffraction Corrections in Radiometry”. J. Opt. Soc. Am., **62**, 9, 1099-1103 (1972).

[7] Boivin L. P., “Diffraction Corrections in Radiometry: comparison of two different methods of calculation”. Applied Optics, **14**, 8, 2002-2009 (1975).

[8] Boivin L. P., "Diffraction Corrections in the radiometry of extended sources". Applied Optics, **15**, 5, 1204-1209 (1976).

[9] Boivin L. P., "Radimetric errors caused by diffraction from circular apertures: edge effects". Applied Optics, **16**, 2, 377-384 (1977).

[10] Eric L. Shirley. "Revised formulas for diffraction effects with point and extended sources". Applied Optics. **37**, 28, 6581-6590 (1998).

[11] E. Wolf. 1955, Proc. Roy. Soc. (A), **230**. 246.

[12] A. Blanc-Lapierre and P. Dumontet, 1955, Rev. d'Optique, **34**, 1.

[13] Gabor, D. J. Inst. Elec. Engrs. London, **93**, 429 (1946).

[14] M. J. Beran and G. B. Parrent. Theory of Partial Coherence. SPIE, Bellingham, (1964). p. 42.

[15] M. Born and E. Wolf. Principles of Optics, Sixth Edition. Pergamon Press, pp 494.

[16] Idem [14]; p. 16.

[17] K. D. Mielenz. ""Wolf Shifts" and Their Physical Interpretation Under Laboratory Conditions". J. Res. Natl. Inst. Stand. Technol. **98**, 231-240 (1993).

[18] Idem [15]; p 435.

[19] Idem [15]; p 438.

[20] Idem [15]; p. 508.

[21] Idem [15]; p. 437.

[22] Idem [14]; p. 104.

[23] K. D. Mielenz. "Monochromator function in partially coherent illumination". J.O.S.A. **57**. 1. 66-74 (1967).

[24] J. G. Suárez. E. Tepichin, K. D. Mielenz. "Cross Spectral Density Propagated Through a Circular Aperture". Metrologia, Cedex, France. (submitted).

[25] A. Papoulis. Systems and Transforms with Application in Optics. McGraw Hill (1968).

[26] J. G. Suárez. E. Tepichin, K. D. Mielenz. "Calculation of the Spectral Radiant Flux Density of a Circular Aperture in the Fresnel Approximation". XVIII congress of ICO, San Francisco, USA (1999).

[27] K. D. Stock, H. Hofer, J. G. Suárez, L. Gonzalez and W. Schmid. "Cryogenic Radiometer Facility of the CENAM and First International Comparison". Procedings 7th International Conference on new Developments and Applications in Optical Radiometry, Spain (1999).

Appendix A

The function $D(v, a, c)$ is defined as

$$D(v,a,c)=\frac{1}{2}T(m_1)+\frac{c^2}{2a^2}T(m_2), \tag{A.1}$$

where

$$m_1=(v^2+a^2-c^2)/2av,$$

$$m_2=(v^2+c^2-a^2)/2cv,$$

and

$$T(x)=2\left[\arccos(x)-x(1-x^2)^{1/2}\right]/p\ . \tag{A.2}$$

$T(x)$ is the optical transfer function for an imaging system with a circular aperture and no aberrations, see reference [6].